ELSEVIER

Physica D 98 (1996) 258–286

PHYSICA D

Long-time effects of bottom topography in shallow water

Roberto Camassa [a,*], Darryl D. Holm [a], C. David Levermore [b]

[a] *Theoretical Division, Los Alamos National Laboratory, Los Alamos, NM 87545, USA*

[b] *Department of Mathematics, University of Arizona, Tucson, AZ 85721, USA*

Abstract

We present and discuss new shallow water equations that provide an estimate of the long-time asymptotic effects of slowly varying bottom topography and weak hydrostatic imbalance on the vertically averaged horizontal velocity of an incompressible fluid with a free surface which is moving under the force of gravity. We consider the regime where the Froude number is much smaller than the aspect ratio δ of the shallow domain. The new equations are obtained at first order in an asymptotic expansion of the solutions of the Euler equations for a shallow fluid by using the small parameter δ^2. The leading order equations in this expansion enforce hydrostatic balance while those obtained at first order retain certain nonhydrostatic effects. Both sets of equations conserve energy and circulation, convect potential vorticity and have a Hamiltonian formulation. The corresponding energy and enstrophy are quadratic integrals with which we can bound the cumulative influence of the nonhydrostatic effects.

Keywords: Shallow water models; Nonhydrostatic topographic effects; Hamiltonian formulation

1. Introduction

Our goal in this paper is to derive model equations that allow us to estimate the effects of slowly varying topography and weak hydrostatic imbalance on the incompressible motion of a shallow inviscid fluid of constant density with a free upper boundary in a gravitational field of intensity g. By using asymptotic expansions, we derive these equations at two successive levels of approximation that share a common Hamiltonian structure leading to a Kelvin circulation theorem, an infinity of integrals of motion, and vortex dynamics analogous to that of the two-dimensional Euler equations for an ideal incompressible fluid. Just as in the two-dimensional Euler equations, the quadratic integrals of motion of these model equations for an ideal fluid – the energy and enstrophy integrals – play a special role.

The fluid is contained in a basin whose fixed lateral boundaries and fixed bottom topography are assumed to vary horizontally in the spatial coordinate $\boldsymbol{x}$ over distances that are large compared to the characteristic depth B. That is, the boundaries of the $\boldsymbol{x}$-domain $\mathcal{D}$ and the fixed bottom topography $z = -b(\boldsymbol{x})$ are assumed to vary slowly with $\boldsymbol{x}$. The mean height of the fluid's free surface is taken to be $z = 0$, so $b(\boldsymbol{x})$ (positive over domain $\mathcal{D}$) is the mean depth of the fluid at position $\boldsymbol{x}$.

* Corresponding author.

0167-2789/96/$15.00 Published by Elsevier Science B.V.
PII S0167-2789(96)00117-0

We consider solutions with horizontal velocity $\boldsymbol{u}$ whose characteristic magnitude U is small compared to the speed of gravity waves $\sqrt{gB}$ and varies horizontally over distances L that are large compared to the characteristic depth B. These solutions have vertical velocities w whose characteristic magnitude W is smaller than U in proportion to the aspect ratio $\delta = B/L$. The amplitude of the deviation of the free surface $z = h(\boldsymbol{x}, t)$ away from its mean value ($z = 0$) is taken to be small compared to B in proportion to the *square* of the "Froude number" $\epsilon = U/\sqrt{gB}$, which is the ratio of the characteristic horizontal fluid speed to the gravity wave speed. Such solutions will evolve over time scales that are long compared to the time for gravity waves to cross the horizontal length scale L in proportion to the reciprocal of the Froude number. In what follows, we develop an asymptotic expansion of the three-dimensional Euler equations and their boundary conditions that involves the dimensionless parameters δ and ϵ, both of which are small compared to unity in such flows.

To leading order in the small dimensionless parameters ϵ and δ, the evolution of the horizontal fluid velocity $\boldsymbol{u}(\boldsymbol{x}, t)$, assumed to be independent of z at leading order, is governed by equations which have the following nondimensional form:

$$\partial_t \boldsymbol{u} + \boldsymbol{u} \cdot \nabla \boldsymbol{u} + \nabla h = 0, \qquad \nabla \cdot (b\boldsymbol{u}) = 0, \tag{1.1}$$

where ∇ is the horizontal gradient and $h(\boldsymbol{x}, t)$ is the leading order amplitude of the free surface. These equations apply to a domain which is shallow compared to its width and whose free surface exhibits negligible wave motion, so we call them the "lake" equations. As we will see, the lake equations are quite robust, as they arise either as the small Froude number limit of the shallow water equations ($\delta \to 0$ first, then $\epsilon \to 0$) or as the long-wave approximation to the rigid lid equations ($\epsilon \to 0$ first, then $\delta \to 0$).

We shall consider the case where $\epsilon \ll \delta$ and carry out the δ-expansion of solutions of the rigid lid equations to the next order, $O(\delta^2)$. At this order, the vertically averaged horizontal fluid velocity, which we also denote by $\boldsymbol{u}(\boldsymbol{x}, t)$, is found to be governed by new asymptotic equations, which we call the "great lake" (GL) equations, that have the nondimensional form

$$\partial_t \boldsymbol{v} + \boldsymbol{u} \cdot \nabla \boldsymbol{v} + (\nabla \boldsymbol{u})\boldsymbol{v} + \nabla \left(h - \tfrac{1}{2}|\boldsymbol{u}|^2\right) = 0, \qquad \nabla \cdot (b\boldsymbol{u}) = 0. \tag{1.2}$$

Here we denote by $(\nabla \boldsymbol{u})\boldsymbol{v} = \sum_{j=1}^{2} v_j \nabla u^j$. The GL equations are written in terms of the auxiliary field $\boldsymbol{v}(\boldsymbol{x}, t)$ defined by

$$\boldsymbol{v} = \boldsymbol{u} + \tfrac{1}{6}\delta^2 b^2 \nabla(\nabla \cdot \boldsymbol{u}). \tag{1.3}$$

Subject to the divergence condition $\nabla \cdot (b\boldsymbol{u}) = 0$, we show that relation (1.3) can be reformulated equivalently as

$$\begin{aligned} b\boldsymbol{v} &\equiv \mathcal{L}(b)\boldsymbol{u} \\ &\equiv b\boldsymbol{u} + \delta^2 \left[-\tfrac{1}{3}\nabla\left(b^3 \nabla \cdot \boldsymbol{u}\right) - \tfrac{1}{2}\nabla\left(b^2 \boldsymbol{u} \cdot \nabla b\right) + \tfrac{1}{2}b^2(\nabla \cdot \boldsymbol{u})\nabla b + b(\boldsymbol{u} \cdot \nabla b)\nabla b\right], \end{aligned} \tag{1.4}$$

where the operator $\mathcal{L}(b)$ is positive-definite (and hence is invertible) provided $b > 0$. Invertibility of the operator $\mathcal{L}(b)$ ensures that $\boldsymbol{u}$ depends continuously on $\boldsymbol{v}$. Moreover, if the bottom is flat, then $\nabla b = 0$ and $\nabla \cdot \boldsymbol{u} = 0$; so these nondimensional equations reduce in this case to the two-dimensional Euler equations for an incompressible fluid with h playing the role of pressure. As in the case of the Euler equations, the pressure h is determined from a Neumann problem that arises from preservation of the (weighted) divergence conditions in (1.2), with tangential boundary conditions on the mean horizontal velocity along the horizontal boundary.

Section 2 derives the GL equations (1.2) in three steps. First, we introduce the small dimensionless parameters δ and ϵ through a dimensional rescaling of the three-dimensional Euler equations and their boundary conditions. Next, we assume that the Froude number is much smaller than the aspect ratio ($\epsilon \ll \delta$) and keep only the leading order terms in ϵ, thereby obtaining a so-called rigid lid approximation. Finally, the solution of the rigid lid equations is expanded asymptotically in δ^2 and it is found that the lake equations (1.1) arise as the leading order balance while the GL equations (1.2) arise at order $O(\delta^2)$. The asymptotic expansion approach, while providing the proper interpretation of the velocity field $\boldsymbol{u}$ as a mean horizontal velocity, also sheds some light on the role of the curl of the auxiliary field $\boldsymbol{v}$, which turns out to be intimately related to a vertical average of the Euler flow's vorticity. Section 3 first shows, by a direct calculation, how the motion governed by the GL equations conserves energy and circulation, and convects a potential vorticity. These results are then rederived in the context of a Hamiltonian formulation for the GL equations. The Hamiltonian for vortex motion is then introduced and stability conditions on steady flows derived via the energy-Casimir method. Section 4 shows that the GL equations can also be understood as the small wave amplitude limit ($\epsilon^2 \to 0$) of the shallow water equations studied by Green and Naghdi [9]. The Green–Naghdi equations retain finite-amplitude gravity waves and their associated Boussinesq-type dispersion properties, which are removed in the GL equations by taking the small amplitude limit. However, the GL equations and Green–Naghdi equations do share the same Lie–Poisson Hamiltonian structure, which leads to many parallels between the two theories. Section 5 provides an example of a steady solution for the lake equations (1.1) that illustrates the influence of bottom topography for the case of irrotational flow. It shows that even in the presence of nonsmooth bottom profile, the leading order equation provides a reasonable approximation for the expected Euler equilibrium flow (with fixed flat surface boundary condition). Section 6 provides an estimate of the maximum rate at which solutions of the model equations at leading order and first order in the asymptotic expansion in δ^2 may deviate from each other. This deviation is measured by the sum of the energy and enstrophy norms of the difference between the solutions of the asymptotic equations at leading order and at first order in the squared aspect ratio δ^2. Our estimate of the deviation of solutions at different asymptotic orders provides analytical information about the sensitivity of the long-time behavior of this shallow water system to the level of approximation used to describe it. Such sensitivity is a classical topic that is finding more and more relevance, for example, in research on assessing the predictability of global ocean modeling. The present work shows that the departure between solutions at leading order and at order $O(\delta^2)$ could grow in time at most exponentially, with an e-folding time scale of L/U, which is the time for a fluid parcel to cross a characteristic horizontal length scale.

2. Derivation of the model equations

2.1. *The scaled Euler equations in three dimensions*

The fluid is assumed to occupy a region defined over a fixed two-dimensional horizontal domain $\mathcal{D}$ that has an outward unit normal $\hat{\boldsymbol{n}}$ on its boundary $\partial\mathcal{D}$. The fixed lateral boundary of the region is assumed to be vertical (i.e., no sloping beaches), and for every $\boldsymbol{x} \in \mathcal{D}$, the fixed bottom is located at $z = -b(\boldsymbol{x})$ while the free top is given by $z = h(\boldsymbol{x}, t)$ (see Fig. 1). Consistency with the definition of h requires that $h(\boldsymbol{x}, t) \geq -b(\boldsymbol{x})$ for every $\boldsymbol{x} \in \mathcal{D}$ and $t \geq 0$.

The motion of an inviscid, incompressible fluid with a free surface moving under gravity with acceleration $-g$ in the z-direction in a three-dimensional domain $\mathcal{D}$ is governed by the Euler equations. We form dimensionless variables in terms of the following natural units: ρ, the mass density; B, the mean depth to the bottom; and $\sqrt{gB}$, the gravity wave speed. We assume that the horizontal length scales are long compared to B by the inverse aspect ratio $1/\delta$, with $\delta \ll 1$, and so, introduce nondimensional spatial variables (adorned with asterisks) by

$$\boldsymbol{x} = (1/\delta)B\boldsymbol{x}^*, \qquad z = Bz^*. \tag{2.1}$$

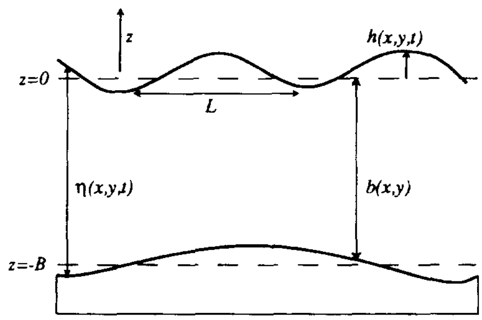

Fig. 1. The set up for lake and GL equations.

We assume that the horizontal fluid speed is small compared to the gravity waves speed $\sqrt{gB}$ by the ratio ϵ, the Froude number, which is also small, $\epsilon \ll 1$. Bearing in mind the aspect ratio, we introduce nondimensional horizontal and vertical velocity fields by

$$\boldsymbol{u} = \epsilon\sqrt{gB}\boldsymbol{u}^*, \qquad w = \delta\epsilon\sqrt{gB}w^*. \tag{2.2}$$

We will work with the modified pressure p (see [2, p. 176]), which is related to the total pressure p_{tot} by $p_{\text{tot}} = p - \rho g z$, that is, p removes the hydrostatic part of the pressure $-\rho g z$ arising from the trivial static solution. The nondimensional surface elevation h^* and (modified) pressure field p^* are

$$h = \epsilon^2 B h^*, \qquad p = \epsilon^2 \rho g B p^*. \tag{2.3}$$

Finally, we introduce a nondimensional temporal variable

$$t = \frac{B}{\delta}\frac{1}{\epsilon\sqrt{gB}}t^*. \tag{2.4}$$

This is the time scale for a fluid parcel to traverse a typical horizontal length, which is long compared to that for a gravity wave to cross a typical horizontal dimension by order $O(1/\epsilon)$. The scaling in Eqs (2.1)–(2.4) selects long-wave (shallow water) motions that evolve slowly with small Froude numbers, of order $O(\epsilon)$, and very small wave amplitudes, of order $O(\epsilon^2)$ compared to the mean depth.

The scaled variables (2.1)–(2.4) yield the following nondimensional form of the motion equations (without asterisks):

$$\partial_t \boldsymbol{u} + \boldsymbol{u}\cdot\boldsymbol{\nabla}\boldsymbol{u} + w\partial_z \boldsymbol{u} + \boldsymbol{\nabla} p = 0, \tag{2.5}$$

$$\delta^2(\partial_t w + \boldsymbol{u}\cdot\boldsymbol{\nabla} w + w\partial_z w) + \partial_z p = 0. \tag{2.6}$$

These nondimensional equations retain their dimensional form except that the vertical acceleration acquires a factor of δ^2; so, the hydrostatic balance condition dominates the vertical motion equation. The nondimensional form of the incompressibility condition acquires no small parameters and all three components of the velocity appear at the same order

$$\boldsymbol{\nabla}\cdot\boldsymbol{u} + \partial_z w = 0. \tag{2.7}$$

The dimensionless boundary conditions acquire factors of the small parameter ϵ^2, as follows. On the free surface we impose the dynamical boundary condition given by

$$p = h \quad \text{for } \boldsymbol{x} \in \mathcal{D} \text{ and } z = \epsilon^2 h(\boldsymbol{x}, t). \tag{2.8}$$

Here, surface tension has been neglected and the ambient pressure is taken to be zero on the surface. Thus, the pressure at the free surface is purely hydrostatic. We assume that no fluid crosses the top, bottom, and lateral boundaries (i.e., that the normal fluid velocity equals the interface velocity), which gives the following kinematic conditions on the velocity components at the top, bottom, and lateral boundaries:

$$w = \epsilon^2(\partial_t h + \boldsymbol{u}\cdot\nabla h) \quad \text{for } \boldsymbol{x}\in\mathcal{D} \text{ and } z = \epsilon^2 h(\boldsymbol{x},t), \tag{2.9}$$

$$w = -\boldsymbol{u}\cdot\nabla b \quad \text{for } \boldsymbol{x}\in\mathcal{D} \text{ and } z = -b(\boldsymbol{x}), \tag{2.10}$$

$$\hat{\boldsymbol{n}}\cdot\boldsymbol{u} = 0 \quad \text{for } \boldsymbol{x}\in\partial\mathcal{D} \text{ and } -b(\boldsymbol{x}) < z < \epsilon^2 h(\boldsymbol{x},t). \tag{2.11}$$

Taken together, conditions (2.9)–(2.11) ensure that the total volume of water remains fixed. This fact allows us to adopt the normalization,

$$\int_{\mathcal{D}} h(\boldsymbol{x},t)\,\mathrm{d}x\,\mathrm{d}y = 0, \tag{2.12}$$

which states that the mean level of the upper water surface is fixed at $z = 0$. Thus, $\epsilon^2 h(\boldsymbol{x},t)$ is the (very small) deviation of the water surface from its mean level, while $b(\boldsymbol{x})$ is the depth of the water basin below the mean level. Thus, we are primarily interested in the case of shallow fluids and very small wave amplitudes, that is,

$$\epsilon \ll \delta \ll 1. \tag{2.13}$$

In this regime, wave effects are neglected. Yet, as we shall see, order δ^2 pressure contributions occur which represent the effects of weakly-broken hydrostatic pressure balance over long times, in the absence of waves.

It will be important in what follows to understand the role of the vorticity field, $(\boldsymbol{\omega},\omega_3) \equiv (\omega_1,\omega_2,\omega_3) = (\partial_y w - \partial_z u_2, \partial_z u_1 - \partial_x w, \partial_x u_2 - \partial_y u_1)$. The scaled coordinates (2.1) and the nondimensional form of the velocity (2.2) suggest to introduce the nondimensional horizontal and vertical vorticity fields as

$$\boldsymbol{\omega} = \epsilon\sqrt{g/B}\,\boldsymbol{\omega}^*, \qquad \omega_3 = \delta\epsilon\sqrt{g/B}\,\omega_3^*. \tag{2.14}$$

Hence, without asterisks, the definition of the nondimensional vorticity field is

$$\omega_1 = \delta^2\partial_y w - \partial_z u_2, \qquad \omega_2 = \partial_z u_1 - \delta^2\partial_x w, \qquad \omega_3 = \partial_x u_2 - \partial_y u_1. \tag{2.15}$$

This nondimensional vorticity is convected by a nondimensional Helmholtz equation where, unlike (2.5) and (2.6), no small parameters appear. Notice, however, that according to (2.15) horizontal variations of the vertical velocity w do acquire the small factor δ^2 in the definition of the horizontal components $\boldsymbol{\omega}$ of vorticity. Thus, the leading order contribution to the horizontal vorticity comes from vertical shears of the horizontal velocity $\boldsymbol{u}$.

2.2. *Leading order models*

In this section we shall consider a long-wave approximation, in the regime $\epsilon \ll \delta$. That is, we shall first consider the nondimensional equations (2.5)–(2.11) in the small Froude number limit of $\epsilon \to 0$ while holding δ fixed and afterwards expand in δ. We have seen that ϵ does not appear at all in the nondimensional equations (2.5)–(2.7). Hence, as $\epsilon \to 0$ the motion equations (2.5) and (2.6) and the incompressibility condition (2.7) remain unchanged. However, ϵ does appear in the rescaled boundary conditions at $O(\epsilon^2)$. Upon letting $\epsilon \to 0$, the dynamic boundary condition (2.8) formally becomes

$$p = h \quad \text{for } \boldsymbol{x}\in\mathcal{D} \text{ and } z = 0, \tag{2.16}$$

while the kinematic boundary conditions (2.9)–(2.11) becomes

$$w = 0 \qquad \text{for } \boldsymbol{x} \in \mathcal{D} \text{ and } z = 0, \tag{2.17}$$

$$w = -\boldsymbol{u} \cdot \boldsymbol{\nabla} b \qquad \text{for } \boldsymbol{x} \in \mathcal{D} \text{ and } z = -b(\boldsymbol{x}), \tag{2.18}$$

$$\hat{\boldsymbol{n}} \cdot \boldsymbol{u} = 0 \qquad \text{for } \boldsymbol{x} \in \partial\mathcal{D} \text{ and } -b(\boldsymbol{x}) < z < 0. \tag{2.19}$$

The system of equations (2.5) with boundary conditions (2.16)–(2.19) is called the "rigid lid" approximation because the horizontal velocity behaves to leading order as if the top surface is fixed at its mean value. However, the designation "rigid" may be misleading here because the leading order behavior of the top surface dynamics is recovered from the dynamic boundary condition (2.16).

The incompressibility condition (2.7) can be integrated in z subject to the top kinematic boundary condition (2.17) to express w in terms of $\boldsymbol{u}$ as

$$w(\boldsymbol{x}, z, t) = \int_z^0 \boldsymbol{\nabla} \cdot \boldsymbol{u}(\boldsymbol{x}, z_1, t)\, \mathrm{d}z_1. \tag{2.20}$$

Then the bottom kinematic boundary condition (2.18) will also be satisfied provided $\boldsymbol{u}$ satisfies the divergence condition

$$\boldsymbol{\nabla} \cdot \left(\int_{-b}^{0} \boldsymbol{u}\, \mathrm{d}z \right) = 0. \tag{2.21}$$

Thus, after first eliminating w by (2.20) and then eliminating p in favor of $\boldsymbol{u}$ and h by integrating (2.6) in z subject to the dynamic boundary condition (2.16), we can consider (2.5) and (2.21) as equations for $\boldsymbol{u}$ and h subject to the boundary condition (2.19).

Formally letting $\delta \to 0$ in the rigid lid equations, (2.5) with boundary conditions (2.16)–(2.19), we express the horizontal velocity $\boldsymbol{u}$, vertical velocity w, pressure p and surface height h as

$$\begin{aligned} \boldsymbol{u} &= \boldsymbol{u}^{(0)} + \mathrm{o}(1), & w &= w^{(0)} + \mathrm{o}(1), \\ p &= p^{(0)} + \mathrm{o}(1), & h &= h^{(0)} + \mathrm{o}(1), \end{aligned} \tag{2.22}$$

and seek equations for $\boldsymbol{u}^{(0)}$, $w^{(0)}$, etc., by requiring that the expansions (2.22) satisfy the rigid lid equations to leading order. The leading order term in the w-equation in (2.6) gives the hydrostatic pressure balance condition

$$\partial_z p^{(0)} = 0, \tag{2.23}$$

which by applying the dynamic boundary condition at the free surface (2.16) relates the pressure to the surface height as

$$p^{(0)} = h^{(0)}(\boldsymbol{x}, t). \tag{2.24}$$

So, hydrostatic balance requires the leading order total pressure $p^{(0)}$ to be independent of the vertical coordinate. The leading order equation for the horizontal motion is

$$\partial_t \boldsymbol{u}^{(0)} + \boldsymbol{u}^{(0)} \cdot \boldsymbol{\nabla} \boldsymbol{u}^{(0)} + w^{(0)} \partial_z \boldsymbol{u}^{(0)} + \boldsymbol{\nabla} h^{(0)} = 0, \tag{2.25}$$

which, after eliminating w by (2.20), will combine with the divergence condition (2.21) and the lateral boundary condition (2.19) to determine $\boldsymbol{u}^{(0)}$ and $h^{(0)}$. Considered as a system, (2.19)–(2.21), and (2.25) constitute the low Froude number limit of the long-wave system of equations studied by Benny [5] and Zakharov [19].

A considerable simplification is achieved by observing that the leading order horizontal motion equation (2.25) may be satisfied by taking the leading order horizontal fluid velocity $\boldsymbol{u}^{(0)}$ to be columnar (independent of the vertical coordinate), so that, like the pressure, it satisfies

$$\partial_z \boldsymbol{u}^{(0)} = 0. \tag{2.26}$$

Because its lateral boundary condition (2.19) contains no explicit z-dependence, the motion equation (2.25) will ensure that no z-dependence will develop in the leading order horizontal velocity provided the initial state is z-independent. This assumption reduces the horizontal motion equation (2.25) and the divergence condition (2.21) to the system

$$\partial_t \boldsymbol{u}^{(0)} + \boldsymbol{u}^{(0)} \cdot \nabla \boldsymbol{u}^{(0)} + \nabla h^{(0)} = 0, \tag{2.27}$$

$$\nabla \cdot \left(b\boldsymbol{u}^{(0)} \right) = 0, \tag{2.28}$$

over the horizontal domain $\mathcal{D}$, while the lateral boundary condition (2.19) becomes

$$\hat{\boldsymbol{n}} \cdot \boldsymbol{u}^{(0)} = 0 \quad \text{for } \boldsymbol{x} \in \partial\mathcal{D}. \tag{2.29}$$

Eqs. (2.27) and (2.28) are the lake equations, which were presented in (1.1) of the introduction without superscripts.

As seen from Eq. (2.15), assumption (2.26) implies that the horizontal vorticity vanishes, $\boldsymbol{\omega}^{(0)} = 0$, at this order. Hence, the Helmholtz equation of vorticity convection reduces at leading order to just a scalar equation for the vertical component

$$\partial_t \omega_3^{(0)} + \boldsymbol{u}^{(0)} \cdot \nabla \omega_3^{(0)} = \omega_3^{(0)} \partial_z w^{(0)} = -\omega_3^{(0)} \nabla \cdot \boldsymbol{u}^{(0)}, \tag{2.30}$$

where

$$\omega_3^{(0)} = \partial_x u_2^{(0)} - \partial_y u_1^{(0)}. \tag{2.31}$$

Upon using the weighted incompressiblity condition (2.28), (2.30) can be written as

$$\left(\partial_t + \boldsymbol{u}^{(0)} \cdot \nabla \right) \left(\omega_3^{(0)}/b \right) = 0, \tag{2.32}$$

that is, the "potential vorticity" $\omega_3^{(0)}/b$ is convected by the leading order system (2.27) and (2.28). The assumption of no vertical shear in the leading order horizontal velocity entails some loss of generality in restricting the initial data for $\boldsymbol{u}^{(0)}$ to be z-independent (2.26). However, this restriction is crucial for the closure scheme derived in Section 2.3.

Given a solution of (2.27)–(2.29) for the leading order horizontal velocity $\boldsymbol{u}^{(0)}$ and free surface $h^{(0)}$ we may recover the leading order vertical velocity $w^{(0)}$ from (2.20) as

$$w^{(0)} = -z \nabla \cdot \boldsymbol{u}^{(0)}. \tag{2.33}$$

Thus, at leading order in the shallow water expansion (2.22) topography appears as a weight factor $b(\boldsymbol{x})$ in the horizontal divergence condition (2.28), the pressure $p^{(0)} = h^{(0)}$ is in hydrostatic balance, and there are no gravity waves.

The lake equations (2.27) and (2.28) could also have been derived by first considering the nondimensional equations (2.5)–(2.11) in the limit of $\delta \to 0$ while holding ϵ fixed and afterwards expanding in ϵ. In this case the first limit corresponds to the usual long-wave (hydrostatic) approximation and, upon assuming the horizontal fluid velocity is columnar, leads to the shallow water equations:

$$\partial_t \boldsymbol{u} + \boldsymbol{u} \cdot \nabla \boldsymbol{u} + \nabla h = 0, \tag{2.34}$$

$$\epsilon^2 \partial_t h + \nabla \cdot \left(\left(b + \epsilon^2 h \right) \boldsymbol{u} \right) = 0, \tag{2.35}$$

over the horizontal domain $\mathcal{D}$, and the boundary condition

$$\hat{\boldsymbol{n}} \cdot \boldsymbol{u} = 0 \quad \text{for } \boldsymbol{x} \in \partial\mathcal{D}. \tag{2.36}$$

Passing to the $\epsilon \to 0$ limit in these equations, one sees that (2.35) becomes the divergence condition (2.28) while the other equations remain unchanged.

The ϵ scaling in the shallow water equations (2.34)–(2.36) is essentially the same scaling used to pass from the compressible Euler equations to the incompressible Euler equations in fluid dynamics (see [3]), where the Mach number plays the same role as the Froude number does here. Just as incompressible fluid dynamics describes the large scale vortical motion of a fluid while suppressing its acoustic waves, the lake equations describe the large scale currents in a body of shallow water while suppressing its gravity waves. Indeed, the well established validity of incompressible fluid dynamics gives us confidence in the validity of not only the lake equations, but also the rigid lid equations, (2.5) with boundary conditions (2.16)–(2.19), which were derived from the Euler equations through a similar scaling and which will be the basis for our subsequent developments.

Given the above observation, the structural similarity of the lake equations (2.27) and (2.28) to the two-dimensional incompressible Euler equations of fluid dynamics is not surprising. Indeed, the motion equation (2.27) is identical to the Euler motion equation with the role of the pressure being played by the free surface height $h^{(0)}$ while the divergence condition (2.28) differs from the Euler incompressibility condition in that it is weighted by the depth $b(\boldsymbol{x})$. As in the Euler case, the free surface height $h^{(0)}$ is determined from the velocity $\boldsymbol{u}^{(0)}$ (tangential to the lateral boundary) by solving a Poisson equation. The Poisson equation appropriate in this case is

$$-\nabla \cdot \left(b \nabla h^{(0)} \right) = \nabla \cdot \left(b \boldsymbol{u}^{(0)} \cdot \nabla \boldsymbol{u}^{(0)} \right), \tag{2.37}$$

which is found by taking the b-weighted divergence of the motion equation (2.27). The boundary condition for the Poisson equation is

$$\hat{\boldsymbol{n}} \cdot \nabla h^{(0)} = -\hat{\boldsymbol{n}} \cdot \left(\boldsymbol{u}^{(0)} \cdot \nabla \boldsymbol{u}^{(0)} \right) \quad \text{for } \boldsymbol{x} \in \partial\mathcal{D}, \tag{2.38}$$

where $\hat{\boldsymbol{n}}$ is the outward unit normal of the boundary $\partial\mathcal{D}$. Together, (2.37) and (2.38) determine $h^{(0)}$ up to an additive constant that is fixed by the h-normalization (2.12).

2.3. Next order model

We now assume $\epsilon \ll \delta$ – corresponding to very small wave amplitudes and very long times – in order to match the next order terms in δ^2 in the rigid lid vertical motion equation (2.6). We expand the dimensionless horizontal velocity $\boldsymbol{u}$, vertical velocity w, pressure p and surface height h in powers of δ^2, as

$$\begin{aligned} \boldsymbol{u} &= \boldsymbol{u}^{(0)} + \delta^2 \boldsymbol{u}^{(1)} + \mathrm{o}(\delta^2), \qquad & w &= w^{(0)} + \delta^2 w^{(1)} + \mathrm{o}(\delta^2), \\ p &= p^{(0)} + \delta^2 p^{(1)} + \mathrm{o}(\delta^2), \qquad & h &= h^{(0)} + \delta^2 h^{(1)} + \mathrm{o}(\delta^2), \end{aligned} \tag{2.39}$$

and seek equations for the coefficients $\boldsymbol{u}^{(0)}$, $\boldsymbol{u}^{(1)}$, etc., by requiring that the expansions in (2.39) satisfy the rigid lid equations and their boundary conditions, at each order in δ^2. With this assumption, the vertical motion equation (2.6) at order $\mathrm{O}(\delta^2)$ yields

$$\partial_z p^{(1)} = -\partial_t w^{(0)} - \boldsymbol{u}^{(0)} \cdot \nabla w^{(0)} - w^{(0)} \partial_z w^{(0)}$$
$$= z \left[\partial_t \nabla \cdot \boldsymbol{u}^{(0)} + \boldsymbol{u}^{(0)} \cdot \nabla \nabla \cdot \boldsymbol{u}^{(0)} - \left(\nabla \cdot \boldsymbol{u}^{(0)} \right)^2 \right] \equiv z p_2^{(1)}. \tag{2.40}$$

Integrating this equation using the dynamic boundary condition (2.16) shows that the pressure at order $O(\delta^2)$ is expressible as

$$p^{(1)} = h^{(1)}(\boldsymbol{x}, t) + \tfrac{1}{2} z^2 p_2^{(1)}(\boldsymbol{x}, t), \tag{2.41}$$

where $p_2^{(1)}$ is given in terms of $\boldsymbol{u}^{(0)}$ by Eq. (2.40).

The horizontal motion equation (2.5) and the divergence condition (2.21) at order $O(\delta^2)$ imply

$$\partial_t \boldsymbol{u}^{(1)} + \boldsymbol{u}^{(0)} \cdot \nabla \boldsymbol{u}^{(1)} + \boldsymbol{u}^{(1)} \cdot \nabla \boldsymbol{u}^{(0)} - \left(\nabla \cdot \boldsymbol{u}^{(0)} \right) z \partial_z \boldsymbol{u}^{(1)} + \nabla h^{(1)} + \tfrac{1}{2} z^2 \nabla p_2^{(1)} = 0, \tag{2.42}$$

$$\nabla \cdot \left(\int_{-b}^{0} \boldsymbol{u}^{(1)} \, \mathrm{d}z \right) = 0, \tag{2.43}$$

while the lateral boundary condition (2.19) implies

$$\hat{\boldsymbol{n}} \cdot \boldsymbol{u}^{(1)} = 0 \quad \text{for } \boldsymbol{x} \in \partial \mathcal{D} \text{ and } -b(\boldsymbol{x}) < z < 0, \tag{2.44}$$

the term $w^{(1)} \partial_z \boldsymbol{u}^{(0)}$ in (2.42) is absent, because the leading order horizontal velocity is columnar, cf. (2.26). Eqs. (2.42)–(2.44) are the $O(\delta^2)$ analog of the lake equations (2.27)–(2.29) and govern the evolution of $\boldsymbol{u}^{(1)}$ and $h^{(1)}$. However, in contrast to what was done at leading order, the first order horizontal velocity $\boldsymbol{u}^{(1)}$ cannot be taken as columnar, in general. Asymptotic solutions of the original three-dimensional incompressible Euler equations with free boundary may be reconstructed in the form (2.39) to order $o(\delta^2)$ from the solutions of these systems with appropriate initial conditions.

For now let us suppose that a solution of the system (2.42)–(2.44) exists. Here we will derive equations for the vertical average of $\boldsymbol{u}^{(1)}$, denoted by

$$\overline{\boldsymbol{u}}^{(1)} \equiv \frac{1}{b} \int_{-b}^{0} \boldsymbol{u}^{(1)} \, \mathrm{d}z. \tag{2.45}$$

Averaging (2.43) and (2.44) gives

$$\nabla \cdot (b \overline{\boldsymbol{u}}^{(1)}) = 0, \tag{2.46}$$
$$\hat{\boldsymbol{n}} \cdot \overline{\boldsymbol{u}}^{(1)} = 0 \quad \text{for } \boldsymbol{x} \in \partial \mathcal{D}. \tag{2.47}$$

An equation for $\overline{\boldsymbol{u}}^{(1)}$ in terms of $\boldsymbol{u}^{(0)}$ can also be obtained by averaging (2.42). Upon computing the averages

$$\frac{1}{b} \int_{-b}^{0} z \partial_z \boldsymbol{u}^{(1)} \, \mathrm{d}z = \boldsymbol{u}^{(1)}\big|_{z=-b} - \overline{\boldsymbol{u}}^{(1)},$$
$$\frac{1}{b} \int_{-b}^{0} \boldsymbol{u}^{(0)} \cdot \nabla \boldsymbol{u}^{(1)} \, \mathrm{d}z = \boldsymbol{u}^{(0)} \cdot \nabla \overline{\boldsymbol{u}}^{(1)} + \frac{\boldsymbol{u}^{(0)} \cdot \nabla b}{b} \left(\overline{\boldsymbol{u}}^{(1)} - \boldsymbol{u}^{(1)}\big|_{z=-b} \right), \tag{2.48}$$

one finds that all instances of $\boldsymbol{u}^{(1)}|_{z=-b}$ in the average of (2.42) cancel and that $\overline{\boldsymbol{u}}^{(1)}$ satisfies

$$\partial_t \overline{\boldsymbol{u}}^{(1)} + \boldsymbol{u}^{(0)} \cdot \nabla \overline{\boldsymbol{u}}^{(1)} + \overline{\boldsymbol{u}}^{(1)} \cdot \nabla \boldsymbol{u}^{(0)} + \nabla h^{(1)} = -\tfrac{1}{6} b^2 \nabla p_2^{(1)}, \tag{2.49}$$

where $p_2^{(1)}$ is expressed in terms of $\boldsymbol{u}^{(0)}$ by (2.40). Although no assumptions were made concerning the vertical dependence of $\boldsymbol{u}^{(1)}$, the result (2.49) is a closed equation for its vertical average $\overline{\boldsymbol{u}}^{(1)}$.

Now we introduce the vertical average of $\boldsymbol{u}$, given by

$$\overline{\boldsymbol{u}} \equiv \frac{1}{b} \int_{-b}^{0} \boldsymbol{u} \, \mathrm{d}z = \boldsymbol{u}^{(0)} + \delta^2 \overline{\boldsymbol{u}}^{(1)} + \cdots \tag{2.50}$$

The divergence condition (2.21) and the boundary condition (2.19) imply together that $\overline{\boldsymbol{u}}$ identically satisfies

$$\nabla \cdot (b \overline{\boldsymbol{u}}) = 0, \tag{2.51}$$

$$\hat{\boldsymbol{n}} \cdot \overline{\boldsymbol{u}} = 0 \quad \text{for } \boldsymbol{x} \in \partial \mathcal{D}. \tag{2.52}$$

It is also easily checked from (2.27) and (2.49) that

$$\partial_t \overline{\boldsymbol{u}} + \overline{\boldsymbol{u}} \cdot \nabla \overline{\boldsymbol{u}} + \nabla h + \delta^2 \left(\partial_t + \overline{\boldsymbol{u}} \cdot \nabla + (\nabla \overline{\boldsymbol{u}}) \right) \left(\tfrac{1}{6} b^2 \nabla (\nabla \cdot \overline{\boldsymbol{u}}) \right) = \mathrm{O}(\delta^4). \tag{2.53}$$

Upon introducing the auxiliary variable $\overline{\boldsymbol{v}}$ by setting

$$\overline{\boldsymbol{v}} = \overline{\boldsymbol{u}} + \tfrac{1}{6} \delta^2 b^2 \nabla (\nabla \cdot \overline{\boldsymbol{u}}), \tag{2.54}$$

Eq. (2.53) takes the more compact form

$$\partial_t \overline{\boldsymbol{v}} + \overline{\boldsymbol{u}} \cdot \nabla \overline{\boldsymbol{v}} + (\nabla \overline{\boldsymbol{u}}) \overline{\boldsymbol{v}} + \nabla \left(h - \tfrac{1}{2} |\overline{\boldsymbol{u}}|^2 \right) = \mathrm{O}(\delta^4). \tag{2.55}$$

Eqs. (2.51), (2.52), and (2.55) are exact counterparts, modulo the unspecified $\mathrm{O}(\delta^4)$ term on the right-hand side of (2.55), of the system of Equations (2.19)–(2.21) and (2.25) with the assumption (2.26).

Exploiting the formal smallness of the $\mathrm{O}(\delta^4)$ term, we now designate by $\boldsymbol{u}$ and h the solution of system (2.51), (2.52), and (2.55) with this term replaced by zero, so that $\boldsymbol{u}$ and h satisfy

$$\partial_t \boldsymbol{v} + \boldsymbol{u} \cdot \nabla \boldsymbol{v} + (\nabla \boldsymbol{u}) \boldsymbol{v} + \nabla \left(h - \tfrac{1}{2} |\boldsymbol{u}|^2 \right) = 0, \tag{2.56}$$

$$\nabla \cdot (b \boldsymbol{u}) = 0, \tag{2.57}$$

over the domain $\mathcal{D}$ subject to the boundary condition,

$$\hat{\boldsymbol{n}} \cdot \boldsymbol{u} = 0 \quad \text{for } \boldsymbol{x} \in \partial \mathcal{D}, \tag{2.58}$$

where the auxiliary field $\boldsymbol{v}$ is related to $\boldsymbol{u}$ by

$$\boldsymbol{v} = \boldsymbol{u} + \tfrac{1}{6} \delta^2 b^2 \nabla (\nabla \cdot \boldsymbol{u}). \tag{2.59}$$

Eqs. (2.56)–(2.58) are the GL equations, which were presented in (1.2). Relation (2.59) is identical to (1.3) and equivalent to (1.4) for those $\boldsymbol{u}$ that satisfy the divergence condition (2.57).

The GL equations (1.2) reduce to the lake equations (1.1) in the limit $\delta \to 0$. The $\mathrm{O}(\delta^2)$ difference between these equations is due to the combined effects of bottom topography and hydrostatic imbalance. We emphasize that bottom topography and hydrostatic imbalance play a combined role. If the bottom is flat, so that ∇b vanishes, then $\nabla \cdot \boldsymbol{u} = 0$

and $\boldsymbol{v}$ reduces to $\boldsymbol{u}$ with no correction for hydrostatic imbalance. In this case, the second order derivative terms in the definition of $\boldsymbol{v}$ in (1.2) vanish entirely, and the lake equations and the GL equations both reduce to the Euler equations for two-dimensional incompressible inviscid flow. Thus, the effects of bottom topography and hydrostatic pressure imbalance are crucially coupled in the asymptotic shallow water expansion (2.39) in the small wave amplitude limit, with $\epsilon = o(\delta)$. We also emphasize that these coupled nonhydrostatic and topographic effects are not to be confused with ordinary Boussinesq-type dispersion of gravity waves, since the wave amplitude *vanishes* at this order in the asymptotics, cf. Section 4, where the comparison with gravity-wave dispersion is discussed further.

We shall analyze the lake and GL systems in the remainder of the paper. The details of the solution for the free surface h from the $\boldsymbol{v}$ equation (2.56), as well as the convection of an appropriately defined vorticity field will be discussed in Section 3.

3. Structure of the GL equations

3.1. Conservation of energy and circulation

The GL equations (2.56)–(2.59) inherit several fundamental properties of the Euler equations. Restoring dimensions in these equations simply removes the δ^2 in Eq. (2.59), the definition of $\boldsymbol{v}$, and replaces h with gh in the motion equation (2.56), yielding

$$\partial_t \boldsymbol{v} + \boldsymbol{u} \cdot \nabla \boldsymbol{v} + (\nabla \boldsymbol{u})\boldsymbol{v} + \nabla \left(gh - \tfrac{1}{2}|\boldsymbol{u}|^2 \right) = 0, \qquad \nabla \cdot (b\boldsymbol{u}) = 0, \tag{3.1}$$

where the auxiliary field $\boldsymbol{v}$ is related to $\boldsymbol{u}$ by

$$\boldsymbol{v} = \boldsymbol{u} + \tfrac{1}{6} b^2 \nabla (\nabla \cdot \boldsymbol{u}). \tag{3.2}$$

The boundary condition (2.58) remains unchanged when dimensions are restored. It is important to note when considering initial data for (3.1) (or even the lake equations) that care must be taken to be sure the data are consistent with the scalings introduced in Section 2, otherwise the resulting solutions could lead to unphysical results such as $h < -b$. This phenomenon will be discussed further in Section 5.

The GL equations inherit the following conserved energy from the Euler equations:

$$E_{\mathrm{GL}} = \tfrac{1}{2} \int \mathrm{d}x\, \mathrm{d}y\, b \left[|\boldsymbol{u}|^2 + \tfrac{1}{3} (\boldsymbol{u} \cdot \nabla b)^2 \right]. \tag{3.3}$$

This is just the expression for the total kinetic energy of the rigid lid equations (2.5) with (2.16)–(2.19),

$$E_{\mathrm{lid}} = \tfrac{1}{2} \int \mathrm{d}x\, \mathrm{d}y \int_{-b}^{0} \mathrm{d}z \left(|\boldsymbol{u}|^2 + w^2 \right), \tag{3.4}$$

when evaluated for a velocity field whose horizontal component $\boldsymbol{u}$ is columnar (2.26) and whose vertical component w is given by (2.20). The conserved energy E_{GL} in (3.3) is a positive-definite quadratic form, expressible more compactly as

$$E_{\mathrm{GL}} = \tfrac{1}{2} \int \mathrm{d}x\, \mathrm{d}y\, b\boldsymbol{u} \cdot \boldsymbol{v}, \tag{3.5}$$

where $\boldsymbol{v}$ is defined by (3.2) and $\nabla \cdot (b\boldsymbol{u}) = 0$ has been used.

The GL equations (3.1) also possess a Kelvin circulation theorem. Specifically, for any closed curve $\gamma(t)$ moving with the fluid, the transport theorem (cf. [2, p. 273]), the Leibnitz identity $\nabla(\boldsymbol{u}\cdot\boldsymbol{v}) = (\nabla\boldsymbol{u})\boldsymbol{v} + (\nabla\boldsymbol{v})\boldsymbol{u}$, and Eq. (3.1) imply that

$$\frac{\mathrm{d}}{\mathrm{d}t}\oint_{\gamma(t)} \boldsymbol{v}\cdot \mathrm{d}\boldsymbol{x} = \oint_{\gamma(t)} [\partial_t \boldsymbol{v} + \boldsymbol{u}\cdot\nabla\boldsymbol{v} - (\nabla\boldsymbol{v})\boldsymbol{u}]\cdot \mathrm{d}\boldsymbol{x}$$
$$= -\oint_{\gamma(t)} \nabla\left(gh - \tfrac{1}{2}|\boldsymbol{u}|^2 + \boldsymbol{u}\cdot\boldsymbol{v}\right)\cdot \mathrm{d}\boldsymbol{x} = 0. \tag{3.6}$$

The GL vorticity Ω is defined to be the curl of the sum of the mean horizontal velocity $\boldsymbol{u}$ plus its correction for hydrostatic imbalance in (3.2). Namely,

$$\Omega \equiv \nabla \times \boldsymbol{v} \equiv \partial_x v_2 - \partial_y v_1. \tag{3.7}$$

The Stokes theorem applied to (3.6) then yields conservation of GL vorticity Ω on fluid parcels,

$$\frac{\mathrm{d}}{\mathrm{d}t}\oint_{\gamma(t)} \boldsymbol{v}\cdot \mathrm{d}\boldsymbol{x} = \frac{\mathrm{d}}{\mathrm{d}t}\int_{\Gamma(t)} \mathrm{d}x\,\mathrm{d}y\,\Omega = 0, \tag{3.8}$$

in which the region $\Gamma(t)$ is enclosed by the curve $\gamma(t)$ moving with the fluid.

Taking the curl of the GL motion equation (3.1) results in an equation for convection of the potential vorticity Ω/b,

$$(\partial_t + \boldsymbol{u}\cdot\nabla)(\Omega/b) = 0. \tag{3.9}$$

At leading order Ω coincides with the vertical component of vorticity, $\omega_3^{(0)}$, and (3.9) consistently reduces to (2.32). At first order, it is shown in [8] that $\Omega = \overline{\omega}_3 - (1/b)\nabla b\cdot\overline{z\omega} + 0(\delta^4)$. By exploiting the formal smallness of the $O(\delta^4)$ term, this now shows that the (three-dimensional) irrotationality of a solution of the original Euler equations (2.5) and (2.6) is reflected by the irrotationality of the auxiliary field $\boldsymbol{v}$, $\nabla\times\boldsymbol{v} = 0$, and *not* by the irrotationality $\nabla\times\boldsymbol{u} = 0$ of a solution of the GL motion equation (2.55). Thus the small extra terms from topography and hydrostatic imbalance in the definition of $\boldsymbol{v}$ are crucial for the correct vorticity budget at the level of approximation of the GL equations (1.2).

Eq. (3.9) is the vorticity stretching relation for the GL equations: when the mean fluid depth b changes, the vorticity Ω changes in proportion. The convection of Ω/b combined with the weighted divergence condition (3.1) and the boundary conditions (2.58) yields an infinity of conserved quantities in the form

$$C_\Phi = \int \mathrm{d}x\,\mathrm{d}y\, b\Phi(\Omega/b), \tag{3.10}$$

for any function Φ.

Note that the conserved energy E_{GL} is a positive-definite quadratic form (3.3) while the potential vorticity Ω/b – being convected – is uniformly bounded by its initial data. These combined features distinguish the GL (and lake) equations from other shallow water equations such as (2.34) and (2.35) and the Green–Naghdi equations (discussed in Section 4). Indeed, the global well-posedness of the GL equations (3.1) has recently been established by combining these energy and vorticity estimates [14], whereas no such result exists for either the shallow water equations (2.34) and (2.35) or the Green–Naghdi equations.

3.2. Hamiltonian formulation

The GL equations (3.1) arise from Hamilton's principle with the following constrained action, which reduces to the kinetic energy (3.3) when evaluated on the constraint manifold $\eta - b = 0$,

$$\mathcal{A}_{\mathrm{GL}} = \frac{1}{2}\int \mathrm{d}t \int \mathrm{d}x\,\mathrm{d}y\left[\eta|\boldsymbol{u}|^2 + \frac{1}{3}\eta^3(\boldsymbol{\nabla}\cdot\boldsymbol{u})^2 + \eta^2(\boldsymbol{\nabla}\cdot\boldsymbol{u})(\boldsymbol{u}\cdot\boldsymbol{\nabla}b) + \eta(\boldsymbol{u}\cdot\boldsymbol{\nabla}b)^2 - 2gh(\eta - b)\right]$$
$$= \int \mathrm{d}t \int \mathrm{d}x\,\mathrm{d}y\left[\frac{1}{2}\boldsymbol{u}\cdot\mathcal{L}(\eta, b)\boldsymbol{u} - gh(\eta - b)\right]. \tag{3.11}$$

Here the operator $\mathcal{L}(\eta, b)$ is given by

$$\mathcal{L}(\eta, b)\boldsymbol{u} = \eta\boldsymbol{u} - \tfrac{1}{3}\boldsymbol{\nabla}(\eta^3\boldsymbol{\nabla}\cdot\boldsymbol{u}) - \tfrac{1}{2}\boldsymbol{\nabla}(\eta^2\boldsymbol{u}\cdot\boldsymbol{\nabla}b) + \tfrac{1}{2}\eta^2(\boldsymbol{\nabla}\cdot\boldsymbol{u})\boldsymbol{\nabla}b + \eta(\boldsymbol{u}\cdot\boldsymbol{\nabla}b)\boldsymbol{\nabla}b, \tag{3.12}$$

and we have used the boundary condition (2.58) in integrating by parts. In (3.11) the surface height h enters the action $\mathcal{A}_{\mathrm{GL}}$ as a Lagrange multiplier which restricts the thickness of the water layer η to equal the equilibrium depth to the bottom $b(\boldsymbol{x})$. The action in (3.11) is similar to the one introduced by Miles and Salmon [16] for the Green–Naghdi equations (see Section 4), but here the gravity waves have been removed entirely by imposing the constraint $\eta = b$ which sets their amplitude to zero.

In expression (3.11) for the GL action, the total fluid depth η and the velocity components u^i $(i = 1,2)$ are given in terms of partial derivatives of the Lagrangian labels, $\tilde{l}^A(\boldsymbol{x}, t)$, which move with the fluid and, thus, satisfy the characteristic equations,

$$\frac{\mathrm{d}\tilde{l}^A}{\mathrm{d}t} \equiv \partial_t\tilde{l}^A + u^i\partial_i\tilde{l}^A = 0, \quad A = 1, 2, \tag{3.13}$$

where $\partial_i = \partial/\partial x^i$ for $i = 1, 2$ and we sum over repeated indices. Incompressibility implies that the (unconstrained) total fluid depth η satisfies

$$\eta = \det\left(\partial_i\tilde{l}^A\right). \tag{3.14}$$

Thus, the fluid depth η is the Jacobian for the transformation from the current Eulerian position x^i to the Lagrangian label $\tilde{l}^A$ with $i, A = 1, 2$. As a consequence of its definition (3.14) and the relation (3.13), the fluid depth η also obeys the continuity equation,

$$\eta_t + \boldsymbol{\nabla}\cdot(\eta\boldsymbol{u}) = 0. \tag{3.15}$$

Consequently, the value $\eta = b(\boldsymbol{x})$ is preserved in time, provided the weighted incompressibility condition in (3.1) is satisfied. In addition, Eq. (3.13) implies the following relation for the horizontal components of the fluid velocity:

$$u^i = -(\tilde{D}^{-1})^i_A\partial_t\tilde{l}^A, \tag{3.16}$$

where the matrix $(\tilde{D}^{-1})^i_A$ is the inverse of the matrix

$$\tilde{D}^A_i \equiv \partial_i\tilde{l}^A. \tag{3.17}$$

The inverse matrix $(\tilde{D}^{-1})^i_A$ exists, since $\det\tilde{D} = \eta \neq 0$, when the constraint is imposed that $\eta = b \neq 0$. Upon using the definitions (3.14) and (3.16) of η and $\boldsymbol{u}$ in terms of $\tilde{l}^A$, and the boundary condition (2.58), the GL equations (3.1) result from stationarity of the action $\mathcal{A}_{\mathrm{GL}}$ in (3.11), under variations with respect to Lagrangian fluid labels $\tilde{l}^A(\boldsymbol{x}, t)$ at fixed Eulerian position and time.

The GL total momentum density $\boldsymbol{\mu}$ is related to the canonical momentum density $\tilde{\pi}_A$, $A = 1, 2$ (obtained from the action principle (3.11) for the GL equations upon varying with respect to $\partial_t \tilde{l}^A$) by

$$\boldsymbol{\mu} = -\tilde{\pi}_A \nabla \tilde{l}^A = \mathcal{L}(\eta, b)\boldsymbol{u}, \tag{3.18}$$

where $\mathcal{L}(\eta, b)$ is defined in Eq. (3.12). Because $\mathcal{L}(\eta, b)$ is invertible provided $\eta > 0$, this relation can be written as

$$\boldsymbol{u} = \mathcal{L}(\eta, b)^{-1}\boldsymbol{\mu}, \tag{3.19}$$

and leads to the remarkable formula,

$$\tilde{\pi}_A \partial_t \tilde{l}^A = \boldsymbol{\mu}\cdot\boldsymbol{u} = \boldsymbol{u}\cdot\mathcal{L}(\eta, b)\boldsymbol{u} = \boldsymbol{\mu}\cdot\mathcal{L}(\eta, b)^{-1}\boldsymbol{\mu}. \tag{3.20}$$

Legendre transforming the GL action (3.11) then gives the constrained Hamiltonian for the GL equations, as

$$H_{\mathrm{GL}} = \int \mathrm{d}x\,\mathrm{d}y \left[\tfrac{1}{2}\boldsymbol{\mu}\cdot\mathcal{L}(\eta, b)^{-1}\boldsymbol{\mu} + gh(\eta - b)\right]. \tag{3.21}$$

Notice that the surface height h is not Legendre-transformed because it has no canonically conjugate momentum. In such cases the constrained Hamiltonian is also known as a Routhian; see [12] for the analogous situation in the case of the incompressible Euler equations. The variational derivatives of H_{GL} with respect to $\boldsymbol{\mu}$ and η are

$$\begin{aligned}
\frac{\delta H_{\mathrm{GL}}}{\delta \boldsymbol{\mu}} &= \boldsymbol{u},\\
\frac{\delta H_{\mathrm{GL}}}{\delta \eta} &= gh - \tfrac{1}{2}|\boldsymbol{u}|^2 - \tfrac{1}{2}\eta^2(\nabla\cdot\boldsymbol{u})^2 - \eta(\nabla\cdot\boldsymbol{u})(\boldsymbol{u}\cdot\nabla b) - \tfrac{1}{2}(\boldsymbol{u}\cdot\nabla b)^2\\
&= gh - \tfrac{1}{2}|\boldsymbol{u}|^2 - \tfrac{1}{2}(\eta\nabla\cdot\boldsymbol{u} + \boldsymbol{u}\cdot\nabla b)^2.
\end{aligned} \tag{3.22}$$

The definitions $\eta = \det(\partial_i \tilde{l}^A)$ and $\boldsymbol{\mu} = -\tilde{\pi}_A \nabla \tilde{l}^A$ allow one to use the chain rule to transform the canonical Poisson bracket in terms of $\tilde{\pi}_A$ and $\tilde{l}^B$, that follows from the GL action principle (3.11),

$$\{F, G\}\left(\tilde{\pi}_A, \tilde{l}^B\right) = -\int \mathrm{d}x\,\mathrm{d}y \left[\frac{\delta F}{\delta \tilde{\pi}_A}\frac{\delta G}{\delta \tilde{l}^A} - \frac{\delta G}{\delta \tilde{\pi}_A}\frac{\delta F}{\delta \tilde{l}^A}\right], \tag{3.23}$$

into the Lie–Poisson bracket in terms of variables $\boldsymbol{\mu}$ and η that is discussed, e.g., in [13]. Namely,

$$\{F, G\}(\boldsymbol{\mu}, \eta) = -\int \mathrm{d}x\,\mathrm{d}y \left[\frac{\delta F}{\delta \mu_i}(\partial_j \mu_i + \mu_j \partial_i)\frac{\delta G}{\delta \mu_j} + \frac{\delta F}{\delta \mu_i}\eta\partial_i\frac{\delta G}{\delta \eta} + \frac{\delta F}{\delta \eta}\partial_j \eta \frac{\delta G}{\delta \mu_j}\right], \tag{3.24}$$

where partial derivatives (e.g., ∂_j) operate on all terms standing to their right. The Lie–Poisson bracket (3.24) satisfies the Jacobi identity,

$$\{E, \{F, G\}\} + \{F, \{G, E\}\} + \{G, \{E, F\}\} = 0, \tag{3.25}$$

simply because it is a variable transform of the Jacobi identity for the canonical Poisson bracket. Lie–Poisson brackets for Eulerian fluid dynamics were first derived by this transformation approach in [11].

The conserved quantitites C_Φ which were defined in (3.10) are the result of substituting the constrained value $\eta = b$ into the so-called "Casimir functionals" for the Lie–Poisson bracket given in (3.24). These functionals, denoted by C_Φ for any function Φ, are given by

$$C_\Phi = \int \mathrm{d}x\,\mathrm{d}y\,\eta\Phi(\Xi/\eta), \tag{3.26}$$

where Ξ is given in terms of μ and η by

$$\Xi \equiv \nabla \times \frac{\mu}{\eta}. \tag{3.27}$$

Note that Ξ reduces to the vorticity Ω, which was defined in (3.7), when the constraint $\eta = b$ is applied. The $\mathcal{C}_\Phi$ are called Casimir functionals for (3.24) because they Poisson-commute with any functional of the variables μ and η under the Lie–Poisson bracket (3.24):

$$\{F, \mathcal{C}_\Phi\}(\boldsymbol{u}, \eta) = 0, \quad \text{for every } F = F(\mu, \eta). \tag{3.28}$$

In particular, they Poisson-commute with the constrained Hamiltonian (3.21); so they are conserved,

$$\frac{\mathrm{d}\mathcal{C}_\Phi}{\mathrm{d}t} = \{\mathcal{C}_\Phi, H_{\mathrm{GL}}\} = 0. \tag{3.29}$$

The Casimirs for a Lie–Poisson dynamical system play a role in assessing the stability of its steady-state solutions (e.g., see [13]), as will be seen later in this section.

The GL equations of motion are expressible in Lie–Poisson Hamiltonian form using the Lie–Poisson bracket (3.24) in terms of μ and η, as

$$\begin{aligned} \partial_t \mu_i &= \{\mu_i, H_{\mathrm{GL}}\} = -(\partial_j \mu_i + \mu_j \partial_i) u^j - \eta \partial_i \frac{\delta H_{\mathrm{GL}}}{\delta \eta}, \\ \partial_t \eta &= \{\eta, H_{\mathrm{GL}}\} = -\partial_j(\eta u^j). \end{aligned} \tag{3.30}$$

Since the depth η satisfies the continuity equation in (3.30), the constrained value $\eta = b$ is invariant, provided the velocity satisfies the weighted incompressibility condition

$$0 = -\partial_j(b u^j). \tag{3.31}$$

Under this condition, Eq. (3.22) yields a simplified expression for $\delta H_{\mathrm{GL}}/\delta\eta$, namely

$$\frac{\delta H_{\mathrm{GL}}}{\delta \eta} = gh - \frac{1}{2}|\boldsymbol{u}|^2, \tag{3.32}$$

and the μ-equation in (3.30) becomes

$$\partial_t \mu_i = -(\partial_j \mu_i + \mu_j \partial_i) u^j - b\partial_i \left(gh - \tfrac{1}{2}|\boldsymbol{u}|^2\right). \tag{3.33}$$

In addition, the quantity $\mu = \mathcal{L}(\eta, b)\boldsymbol{u}$ with $\eta = b$ now reduces to

$$\mu \equiv \mathcal{L}(b)\boldsymbol{u} = b\boldsymbol{u} - \tfrac{1}{3}\nabla(b^3 \nabla \cdot \boldsymbol{u}) - \tfrac{1}{2}\nabla(b^2 \boldsymbol{u} \cdot \nabla b) + \tfrac{1}{2} b^2 (\nabla \cdot \boldsymbol{u}) \nabla b + b(\boldsymbol{u} \cdot \nabla b)\nabla b. \tag{3.34}$$

Using $\nabla \cdot (b\boldsymbol{u}) = 0$, this becomes

$$\mu = \mathcal{L}(b)\boldsymbol{u} = b\boldsymbol{u} + \tfrac{1}{6} b^3 \nabla(\nabla \cdot \boldsymbol{u}) = b\boldsymbol{v}, \tag{3.35}$$

where $\boldsymbol{v}$ is given in (3.2). After a short manipulation Eqs. (3.31) and (3.33) recover the GL equations (3.1), now derived from the action principle (3.11) and cast into Lie–Poisson Hamiltonian form (3.30) with the constrained Hamiltonian (or Routhian) (3.21).

The operator $\mathcal{L}(b)$ in Eq. (3.34) is elliptic and self-adjoint. It is also positive-definite and therefore invertible, provided the depth b is not identically zero. The operator $\mathcal{L}(b)$ also figures in the solution for the pressure p from the $\boldsymbol{v}$ equation (3.1). Operating on this equation with $\nabla \cdot b\mathcal{L}^{-1}(b)b$ and using weighted incompressibility gives an elliptic equation for the pressure which is reminiscent of the Poisson equation for the pressure in the case of the Euler equations, namely

$$\nabla \cdot \left(b\mathcal{L}(b)^{-1}\left[b\left(\nabla(gh - \tfrac{1}{2}|\boldsymbol{u}|^2) + \boldsymbol{u}\cdot\nabla\boldsymbol{v} + (\nabla\boldsymbol{u})\boldsymbol{v}\right)\right]\right) = 0. \tag{3.36}$$

The corresponding lateral boundary condition is

$$\hat{\boldsymbol{n}} \cdot \left(b\mathcal{L}(b)^{-1}\left[b\left(\nabla(gh - \tfrac{1}{2}|\boldsymbol{u}|^2) + \boldsymbol{u}\cdot\nabla\boldsymbol{v} + (\nabla\boldsymbol{u})\boldsymbol{v}\right)\right]\right) = 0, \quad \text{on } \partial\mathcal{D}, \tag{3.37}$$

where $\hat{\boldsymbol{n}}$ is the outward unit normal of the boundary $\partial\mathcal{D}$. Together, (3.36) and (3.37) determine h up to an additive constant that is fixed by the h-normalization (2.12).

3.3. Hamiltonian vortex dynamics

The general solution $\boldsymbol{u}$ of the divergence condition in (3.1) can be expressed in terms of a stream function ψ as

$$b\boldsymbol{u} = (-\partial_y\psi, \partial_x\psi). \tag{3.38}$$

The boundary condition (2.58) implies the stream function takes a constant value on each connected component of the boundary $\partial\mathcal{D}$ of the domain of flow. When $\partial\mathcal{D}$ has just one connected component the value of the stream function on the boundary $\psi|_{\partial\mathcal{D}}$ can be taken to be zero.

The stream function ψ is related to the vorticity Ω by the negative-definite operator $\mathcal{S}(b)$ given by

$$\Omega = \mathcal{S}(b)\psi \equiv \nabla\cdot\left(\frac{1}{b}\nabla\psi\right) - \frac{1}{6}\left[b^2, \left[\frac{1}{b}, \psi\right]\right], \tag{3.39}$$

in which the square brackets are defined for functions σ, ζ of coordinates x, y to be

$$[\sigma, \zeta] \equiv \partial_x\sigma\partial_y\zeta - \partial_y\sigma\partial_x\zeta \equiv \nabla\sigma \times \nabla\zeta. \tag{3.40}$$

Thus, $[\sigma, \zeta]$ is the (x, y) Jacobian determinant of σ and ζ. The operator $\mathcal{S}(b)$ in (3.39) is elliptic, and is invertible, provided the depth b is positive.

Assuming $\partial\mathcal{D}$ has only one connected component and thereby taking $\psi|_{\partial\mathcal{D}} = 0$, the GL energy E_{GL} in (3.5) is expressible in terms of the scalar vorticity Ω as

$$\begin{aligned} E_{GL} &= \frac{1}{2}\int \mathrm{d}x\,\mathrm{d}y\, b\boldsymbol{u}\cdot\boldsymbol{v} \\ &= -\frac{1}{2}\int \mathrm{d}x\,\mathrm{d}y\,\psi\Omega + \frac{1}{2}\psi|_{\partial\mathcal{D}}\oint_{\partial\mathcal{D}} \boldsymbol{v}\cdot\mathrm{d}\boldsymbol{x} = -\frac{1}{2}\int \mathrm{d}x\,\mathrm{d}y\,\psi\Omega. \end{aligned} \tag{3.41}$$

If $\partial\mathcal{D}$ were to have more than one connected component, the constant values of $\psi|_{\partial\mathcal{D}}$ on each component of $\partial\mathcal{D}$ could be regarded as Lagrange multipliers enforcing constancy of the circulation (by Kelvin's theorem) on that component (e.g., see [13]).

The GL dynamics can be given an alternative Hamiltonian form upon defining a Lie–Poisson bracket by

$$\{F, G\} = \int \mathrm{d}x\,\mathrm{d}y \frac{\Omega}{b}\left[\frac{\delta F}{\delta\Omega}, \frac{\delta G}{\delta\Omega}\right], \tag{3.42}$$

and setting the Hamiltonian H to be E_{GL} as expressed in (3.41). Upon integrating by parts and using

$$\delta H/\delta\Omega = -\mathcal{S}^{-1}(b)\Omega = -\psi,$$

the advection equation for Ω/b is thereby recovered as

$$\partial_t \Omega = \{\Omega, H\} = \left[\frac{\delta H}{\delta \Omega}, \frac{\Omega}{b}\right] = \nabla\psi \times \nabla\left(\frac{\Omega}{b}\right) = -b\boldsymbol{u}\cdot\nabla\left(\frac{\Omega}{b}\right). \tag{3.43}$$

The conserved quantities C_Φ in (3.10) satisfy

$$\{C_\Phi, F\} = 0, \quad \text{for every } F = F(\Omega), \tag{3.44}$$

and are thereby Casimirs for the Lie–Poisson bracket (3.42). In contrast to the previous Hamiltonian structure associated with (3.24), this structure does not require the imposition of a constraint.

For each Casimir C_Φ the critical points Ω_e of the functional $H_\Phi \equiv H + C_\Phi$, which satisfy

$$\delta H_\Phi(\Omega_e) = 0, \tag{3.45}$$

are steady GL flows, that satisfy

$$[\psi_e, \Omega_e/b] = b\boldsymbol{u}_e \cdot \nabla(\Omega_e/b) = 0. \tag{3.46}$$

To show that critical points of H_Φ correspond to steady flows, we compute, for an arbitrary function $\delta\Omega$, the first variation of H_Φ

$$\delta H_\Phi(\Omega) = \int \mathrm{d}x\,\mathrm{d}y\,[-\psi + \Phi'(\Omega/b)]\delta\Omega. \tag{3.47}$$

Thus, criticality of H_Φ at Ω_e implies the relation

$$\psi_e = \Phi'(\Omega_e/b), \tag{3.48}$$

which certainly satisfies (3.46). Consequently, each function Φ in the Casimir (3.10) corresponds to a steady flow of the GL equations.

3.4. Stability of steady flows

The stability of a steady GL flow satisfying (3.48) may be determined by inquiring whether the quadratic form $\delta^2 H_\Phi(\Omega_e)$ given by the second variation of H_Φ evaluated at the equilibrium solution Ω_e is definite in sign. The quadratic form $\delta^2 H_\Phi(\Omega_e)$ is the conserved Hamiltonian for the linearized motion around the equilibrium solution Ω_e, for which $\delta H_\Phi(\Omega_e) = 0$. Definiteness of this quadratic form assures the existence of a norm which remains constant under the linearized motion, providing so-called linear Lyapunov stability of the flow (see [13]). The condition for such definiteness is easily expressible in terms of the second derivative $\Phi''(\Omega_e/b)$ and the spectrum of the operator $-b^{-1}\mathcal{S}(b)$. By direct computation we have

$$\delta^2 H_\Phi(\Omega_e) = \int b^{-1}\,\mathrm{d}x\,\mathrm{d}y\,\delta\Omega\left[-b\mathcal{S}^{-1}(b) + \Phi''(\Omega_e/b)\right]\delta\Omega. \tag{3.49}$$

Since the operator $-b\mathcal{S}^{-1}(b)$ is positive-definite, we immediately have

$$\delta^2 H_\Phi(\Omega_e) \geq 0, \quad \text{provided } \Phi''(\Omega_e/b) > 0, \tag{3.50}$$

with equality occurring if and only if $\delta\Omega = 0$. By (3.48) the second derivative $\Phi''(\Omega_e/b)$ corresponds to the following ratio, from (3.48):

$$\Phi''(\Omega_e/b) = \frac{\mathrm{d}\psi_e}{\mathrm{d}(\Omega_e/b)}. \tag{3.51}$$

Now, suppose the bottom topography b is such that the spectrum of $-b^{-1}\mathcal{S}(b)$ is bounded away from zero, and ordered according to

$$0 < \lambda_1 < \lambda_2 < \lambda_3 < \cdots \tag{3.52}$$

Then in terms of the pairing

$$(\phi, \psi) = \int \mathrm{d}x\,\mathrm{d}y b^{-1}\phi\psi, \tag{3.53}$$

we may define an orthonormal basis with weight function b^{-1} and write

$$(\phi, -b^{-1}\mathcal{S}(b)\phi) = \sum \lambda_n |\phi_n|^2 \geq \lambda_1 \sum |\phi_n|^2. \tag{3.54}$$

So,

$$(\phi, -b\mathcal{S}^{-1}(b)\phi) \leq (1/\lambda_1)(\phi, \phi) \tag{3.55}$$

and

$$\delta^2 H_\Phi(\Omega_e) \leq \int \mathrm{d}x\,\mathrm{d}y\, b^{-1}\delta\Omega \left[\frac{1}{\lambda_1} + \Phi''(\Omega_e/b)\right]\delta\Omega. \tag{3.56}$$

Summarizing, the second variation evaluated at the equilibrium $\delta^2 H_\Phi(\Omega_e)$ is definite in sign, provided

$$\Phi''(\Omega_e/b) > 0, \quad \text{so that } \delta^2 H_\Phi(\Omega_e) > 0,$$

or

$$\Phi''(\Omega_e/b) < -1/\lambda_1, \quad \text{so that } \delta^2 H_\Phi(\Omega_e) < 0. \tag{3.57}$$

Linear Lyapunov stability now follows for GL equilibria that satisfy one of the stability conditions (3.57).

For example, consider an equilibrium shear flow in the x-direction with fluid velocity $\boldsymbol{u}_e = (U(y), 0) = (-\psi_2'/b, 0)$ and topography $b(y)$ each depending only on the coordinate in the spanwise direction, y. For such an equilibrium flow we have

$$\frac{\Omega_e}{b} = -\frac{U'(y)}{b(y)}, \tag{3.58}$$

so that

$$\nabla\left(\frac{\Omega_e}{b}\right) = -\left(\frac{U'(y)}{b(y)}\right)'\hat{\boldsymbol{y}}. \tag{3.59}$$

Consequently, cf. Eq. (3.51),

$$\Phi''(\Omega_e/b) = \frac{bU(y)}{(U'(y)/b(y))'}. \tag{3.60}$$

Perhaps not unexpectedly, when b =const., the stability condition $\Phi''(\Omega_e/b) > 0$ in (3.57) reduces to Rayleigh's inflection point criterion for two-dimensional incompressible shear flows. That is, a plane parallel incompressible flow with no inflection point in its velocity profile is linearly stable. By (3.60), the effect of topography for such flows may be either stabilizing (in which case an inflection point may be allowed in the velocity profile without destroying stability), or destabilizing (in which case a shear flow without an inflection point in its velocity profile may still violate the stability condition (3.57)).

Notice that the expression (3.60) is independent of the aspect ratio δ, so it applies to both lake and GL equilibria. The stability criteria (3.57) for linear Lyapunov stability of equilibrium shear flow solutions of the lake and GL equations may be promoted to criteria for their nonlinear Lyapunov stability by requiring convexity of the function $\Phi(\Omega_e/b)$, in analogy with the results of Arnold [1] for incompressible planar flows.

4. Relation to the Green–Naghdi model

4.1. Green–Naghdi equations

This section discusses the relation between the GL equations (3.1) and the Green–Naghdi (GN) equations [9] for nonlinearly dispersive gravity waves in shallow water. The GN equations are (in dimensional form)

$$\partial_t \boldsymbol{u} = -\boldsymbol{u}\cdot\nabla\boldsymbol{u} - g\nabla(\eta - b) + (1/\eta)\nabla A + (1/\eta)B\nabla b, \qquad \partial_t\eta = -\nabla\cdot(\eta\boldsymbol{u}), \tag{4.1}$$

where $\eta = h(\boldsymbol{x},t) + b(\boldsymbol{x})$ is the local depth of the water. The quantities A and B are given by

$$A = \eta^2\frac{\mathrm{d}}{\mathrm{d}t}\left(\tfrac{1}{3}\eta\nabla\cdot\boldsymbol{u} + \tfrac{1}{2}\boldsymbol{u}\cdot\nabla b\right), \qquad B = -\eta\frac{\mathrm{d}}{\mathrm{d}t}\left(\tfrac{1}{2}\eta\nabla\cdot\boldsymbol{u} + \boldsymbol{u}\cdot\nabla b\right), \tag{4.2}$$

and $\mathrm{d}/\mathrm{d}t = \partial_t + \boldsymbol{u}\cdot\nabla$ is the material derivative following the horizontal velocity, $\boldsymbol{u}$. The GN equations provide a vertically averaged description of shallow water motion with a free surface under gravity. These equations were derived in the setting of one horizontal dimension and a flat bottom by Su and Gardner [18] as a dispersive correction to the usual shallow water equations. They were derived in the more general setting used here by Green and Naghdi [9] by requiring the incompressible columnar motion to satisfy conservation of energy and invariance under rigid body translations. They were then rediscovered by Bazdenkov et al. [4], who also considered the case of a rotating frame. Finally, they were derived from a variational principle by Miles and Salmon [16] by inserting the columnar motion solution ansatz into the variational principle for the Euler equations for an inviscid incompressible fluid, and explicitly performing the vertical integrations before varying.

The GN equations retain finite-amplitude gravity waves and their associated Boussinesq-type dispersion properties, which are neglected in the GL equations on taking the small amplitude limit ($\epsilon^2 \to 0$). We show here that the GL equations can be understood as the small wave amplitude limit of the GN equations. In fact, we could have derived the GN equations as an intermediate step in our asymptotic expansion for the Euler equations in Section 2, by *not* imposing small Froude number (and, thus, small wave amplitude). The GL and the GN equations turn out to share similar Lie–Poisson Hamiltonian structures, leading to many parallels between the two theories and, thus, suggesting new results for the GN theory as well.

The global well-posedness of the GL equations has recently been established in [14]. This result provides a foundation for a rigorous justification of the formal derivation of the GL equations given in Section 3. From our viewpoint, it is worthwhile to make the connection between the GL equations and the GN equations, because the global well-posedness of the GL equations validates the use of the GN equations over long times, in the limit of small wave amplitude. No such result exists for the GN equations. For finite wave amplitudes, a numerical comparison of the GN equations with the Euler equations for finite wave amplitude free surface incompressible flow over bottom topography has recently been discussed by Margolin et al. [15]. This reference shows that numerical simulations of the GN equations tend to be faithful representations of the corresponding Euler solutions, so long as wave breaking does not occur.

The GN equations (4.1) and (4.2) can assume a different form, one which is more natural from a variational standpoint and which is similar to that of the GL equations (3.1). Using the operator $\mathcal{L}(\eta, b)$ defined in (3.12) and introducing the auxiliary field

$$\eta \boldsymbol{v}_{\mathrm{GN}} \equiv \mathcal{L}(\eta, b)\boldsymbol{u}, \tag{4.3}$$

the first equation in the GN system (4.1) and (4.2) can be rewritten (using the second equation in (4.1) and judiciously differentiating by parts) in the form

$$\begin{aligned} &\partial_t \boldsymbol{v}_{\mathrm{GN}} + \boldsymbol{u}\cdot\nabla\boldsymbol{v}_{\mathrm{GN}} + (\nabla\boldsymbol{u})\boldsymbol{v}_{\mathrm{GN}} \\ &\quad + \nabla\left(g(\eta-b) - \tfrac{1}{2}|\boldsymbol{u}|^2 - \tfrac{1}{2}(\eta\nabla\cdot\boldsymbol{u} + \boldsymbol{u}\cdot\nabla b)^2\right) = 0. \end{aligned} \tag{4.4}$$

The GL equations (3.1) now follow immediately from this form of the GN equations by formally taking the asymptotic limit $\epsilon \to 0$ after the rescaling in which

$$\nabla \to \nabla, \qquad \partial_t \to \epsilon\partial_t, \qquad \boldsymbol{u} \to \epsilon\boldsymbol{u}, \qquad \eta \to b + \epsilon^2 h, \tag{4.5}$$

so that

$$\begin{aligned} &g(\eta-b) \to \epsilon^2 gh, \qquad \mathcal{L}(\eta, b) \to \mathcal{L}(b) + \mathrm{O}(\epsilon^2), \\ &(\eta\nabla\cdot\boldsymbol{u} + \boldsymbol{u}\cdot\nabla b)^2 \to (\nabla\cdot(b\boldsymbol{u}))^2 + \mathrm{O}(\epsilon^2). \end{aligned}$$

The rescaled GN equations in this small-Froude-number limit reduce to the system

$$\begin{aligned} &\partial_t \boldsymbol{v}_{\mathrm{GN}} + \boldsymbol{u}\cdot\nabla\boldsymbol{v}_{\mathrm{GN}} + (\nabla\boldsymbol{u})\boldsymbol{v}_{\mathrm{GN}} + \nabla\left(gh - \tfrac{1}{2}|\boldsymbol{u}|^2\right) = \mathrm{O}(\epsilon^2), \\ &\nabla\cdot(b\boldsymbol{u}) = \mathrm{O}(\epsilon^2), \qquad b\boldsymbol{v}_{\mathrm{GN}} = \mathcal{L}(b)\boldsymbol{u} + \mathrm{O}(\epsilon^2). \end{aligned} \tag{4.6}$$

where $\mathcal{L}(b)$ is given in Eq. (3.34). When the $\mathrm{O}(\epsilon^2)$ terms are dropped, we see that this asymptotic limit of the GN equations (4.1), which corresponds to looking at small surface height displacements over long-time scales, reduces to the GL equations (3.1).

4.2. *The Hamilton principle for the GN equations*

The approach of Miles and Salmon [16] in recovering the GN equations by restricting to columnar motion in the Hamilton principle for an incompressible fluid with a free surface affords a convenient starting point for deriving the Lie–Poisson Hamiltonian structure of these equations which has already been discussed in [10]. The three-dimensional Euler equations, (2.5) and (2.6) with dimensions restored (i.e., suppressing δ), follow from an action principle $\delta\mathcal{A} = 0$, with

$$\mathcal{A} = \int \mathrm{d}t \int \mathrm{d}x\,\mathrm{d}y \int_{-b}^{h} \mathrm{d}z\, D\left[\tfrac{1}{2}(\boldsymbol{u}^2 + w^2) - gz - p(D^{-1} - 1)\right], \tag{4.7}$$

where $D = \det(D_i^A)$, where $D_i^A = (\partial l^A/\partial x^i)$ is the 3×3 Jacobian matrix for the map from Eulerian coordinates to Lagrangian fluid labels, $l^A(\boldsymbol{x}, z, t)$, $A = 1, 2, 3$. These Lagrangian labels specify the fluid particle currently occupying Eulerian position $(x^1, x^2, x^3) = (\boldsymbol{x}, z)$. They satisfy the advection law, $0 = \mathrm{d}l^A/\mathrm{d}t = \partial l^A/\partial t + u^i D_i^A + w D_3^A$, thereby determining the velocity components $(\boldsymbol{u}, w)$ in the action principle, as

$$u^i = -(D^{-1})^i_A \partial_t l^A, \quad i = 1, 2, \qquad w = -(D^{-1})^3_A \partial_t l^A. \tag{4.8}$$

where, as usual, we sum on repeated indices. Variations in (4.7) with respect to l^A yield the Euler equations for kinematic boundary conditions (2.9)–(2.11), with dimensions restored (i.e., suppressing ϵ). The constraint $D = 1$ imposed by the Lagrange multiplier p (the pressure) implies incompressibility. For more details, see [12,16].

Miles and Salmon [16] find an action principle for the GN equations, by restricting the action principle (4.7) to variations of the form (columnar motion ansatz)

$$l^A = \tilde{l}^A(\boldsymbol{x}, t), \quad A = 1, 2,$$
$$l^3 = \tilde{l}^3 = (z + b)/(h + b), \tag{4.9}$$

from which (4.8) implies

$$\boldsymbol{u} = \boldsymbol{u}(\boldsymbol{x}, t) \quad \text{and} \quad w = -z\boldsymbol{\nabla} \cdot \boldsymbol{u} - \boldsymbol{\nabla} \cdot (b\boldsymbol{u}). \tag{4.10}$$

For restricted variations of this type, Miles and Salmon [16] show that after performing the vertical integrations the action (4.7) reduces to (cf. $\mathcal{A}_{\mathrm{GL}}$ in Eq. (3.11))

$$\mathcal{A}_{\mathrm{GN}} = \frac{1}{2}\int \mathrm{d}t \int \mathrm{d}x\,\mathrm{d}y \left[\eta|\boldsymbol{u}|^2 + \tfrac{1}{3}\eta^3(\boldsymbol{\nabla}\cdot\boldsymbol{u})^2 + \eta^2(\boldsymbol{\nabla}\cdot\boldsymbol{u})(\boldsymbol{u}\cdot\boldsymbol{\nabla}b) + \eta(\boldsymbol{u}\cdot\boldsymbol{\nabla}b)^2 - g(\eta - b)^2\right], \tag{4.11}$$

where we have from incompressibility,

$$D = \det(D_i^A) = 1 \quad \Rightarrow \quad \det\left(\partial_i \tilde{l}^A\right) = \left(\partial_z \tilde{l}^3\right)^{-1} = \eta, \tag{4.12}$$

and from advection of the fluid labels,

$$\partial_t \tilde{l}^A = -\boldsymbol{u} \cdot \boldsymbol{\nabla} \tilde{l}^A \quad \Rightarrow \quad u^i = -\frac{\partial x^i}{\partial \tilde{l}^A}\partial_t \tilde{l}^A, \quad i, A = 1, 2. \tag{4.13}$$

The GN equations (4.4) then result from stationarity of the action $\mathcal{A}_{\mathrm{GN}}$ under variations with respect to Lagrangian fluid labels $\tilde{l}^A(\boldsymbol{x}, t)$ at fixed Eulerian position and time. The similarity of the action $\mathcal{A}_{\mathrm{GN}}$ for the GN equations to the action $\mathcal{A}_{\mathrm{GL}}$ in Eq. (3.11) for the GL equations makes it possible to transfer many of the results of Section 3 for GL immediately over to the GN case.

4.3. Hamiltonian structure for the GN equations

Passing from the Miles–Salmon action principle (4.11) for the GN equations via the same Legendre transformation as in Section 3 using Eq. (3.20) yields the corresponding GN Hamiltonian. In terms of the variables $\boldsymbol{\mu}$ and η, defined as before by

$$\boldsymbol{\mu} = -\tilde{\pi}_A \boldsymbol{\nabla} \tilde{l}^A = \mathcal{L}(\eta, b)\boldsymbol{u} \quad \text{and} \quad \eta = \det\left(\partial_i \tilde{l}^A\right), \tag{4.14}$$

the resulting GN Hamiltonian is expressible as

$$H_{\mathrm{GN}} = \frac{1}{2}\int \mathrm{d}x\,\mathrm{d}y \left[\boldsymbol{\mu} \cdot \mathcal{L}(\eta, b)^{-1}\boldsymbol{\mu} + g(\eta - b)^2\right]. \tag{4.15}$$

This is the sum of the kinetic and gravitational potential energies of the fluid (cf. the constrained Hamiltonian H_{GL} in Eq. (3.21)). As discussed earlier, the operator $\mathcal{L}(\eta, b)$ is positive-definite, self-adjoint, one-to-one and its inverse exists, provided $\eta > 0$. The variational derivatives of H_{GN} in Eq. (4.15) are given by (cf. Eq. (3.22))

$$\frac{\delta H_{\mathrm{GN}}}{\delta \boldsymbol{\mu}} = \boldsymbol{u}, \qquad \frac{\delta H_{\mathrm{GN}}}{\delta \eta} = g(\eta - b) - \tfrac{1}{2}|\boldsymbol{u}|^2 - \tfrac{1}{2}(\eta\boldsymbol{\nabla}\cdot\boldsymbol{u} + \boldsymbol{u}\cdot\boldsymbol{\nabla}b)^2. \tag{4.16}$$

The definitions (4.14) allow us to pass again from the canonical Poisson bracket (3.23) to the Lie–Poisson bracket (3.24), by a change of variables in the *same* form as for the GL theory. The corresponding equations of motion are given in Lie–Poisson Hamiltonian form by (cf. Eqs. (3.30))

$$\begin{aligned}\frac{\partial \mu_i}{\partial t} &= \{\mu_i, H_{\mathrm{GN}}\} = -(\partial_j \mu_i + \mu_j \partial_i) u^j - \eta \partial_i \frac{\delta H_{\mathrm{GN}}}{\delta \eta},\\ \frac{\partial \eta}{\partial t} &= \{\eta, H_{\mathrm{GN}}\} = -\partial_j (\eta u^j).\end{aligned} \tag{4.17}$$

These are the GN equations (4.1) (see also (4.4)), expressed in the Lie–Poisson Hamiltonian form in terms of $\boldsymbol{\mu}$ and η given previously in [10].

4.4. GN circulation theorems

The Hamiltonian equations (4.17) suggest rewriting the GN equations in vector form as

$$\partial_t \boldsymbol{v}_{\mathrm{GN}} + \boldsymbol{u} \cdot \boldsymbol{\nabla} \boldsymbol{v}_{\mathrm{GN}} + (\boldsymbol{\nabla} \boldsymbol{u}) \boldsymbol{v}_{\mathrm{GN}} + \boldsymbol{\nabla}(\delta H_{\mathrm{GN}}/\delta \eta) = 0, \qquad \partial_t \eta + \boldsymbol{\nabla} \cdot (\eta \boldsymbol{u}) = 0, \tag{4.18}$$

where $\boldsymbol{v}_{\mathrm{GN}} = \boldsymbol{\mu}/\eta$ (cf. (3.35)). Consequently, the GN equations have a Kelvin circulation theorem (cf. Eq. (3.6) for the GL equations), namely

$$\frac{\mathrm{d}}{\mathrm{d}t} \oint_{\gamma(t)} \boldsymbol{v}_{\mathrm{GN}} \cdot \mathrm{d}\boldsymbol{x} = 0. \tag{4.19}$$

Introducing the GN vorticity

$$\Omega_{\mathrm{GN}} \equiv \boldsymbol{\nabla} \times \boldsymbol{v}_{\mathrm{GN}}, \tag{4.20}$$

then taking the curl of the GN motion equation in (4.18) and using the continuity equation for η implies local advection of the potential vorticity $\Omega_{\mathrm{GN}}/\eta$, namely

$$(\partial_t + \boldsymbol{u} \cdot \boldsymbol{\nabla})(\Omega_{\mathrm{GN}}/\eta) = 0. \tag{4.21}$$

This is the vortex stretching relation for the GN equations: when the fluid depth η changes, the vorticity changes in proportion. Here vorticity Ω_{GN} is the curl of the total specific momentum of the flow.

One drawback of the derivation of the GN equations via an action principle may now be noticed. According to the columnar motion ansatz (4.10), the vertical component of vorticity should be $\hat{z} \cdot (\boldsymbol{\nabla} \times \boldsymbol{u})$. Thus, irrotational solutions of Euler equations, e.g., for flows originating from rest, would imply $\hat{z} \cdot (\boldsymbol{\nabla} \times \boldsymbol{u}) = 0$ during the motion, whereas the definitions (4.20), (3.12) and Eq. (4.21) show that this cannot be the case. In fact, Miles and Salmon [16] remark that the GN equations exhibit a source of vorticity

$$-(\partial_t + \boldsymbol{u} \cdot \boldsymbol{\nabla}) \left(\frac{\Omega^*_{\mathrm{GN}}}{\eta} \right) \equiv (\partial_t + \boldsymbol{u} \cdot \boldsymbol{\nabla}) \left(\frac{\boldsymbol{\nabla} \times (\boldsymbol{u} - \boldsymbol{v}_{\mathrm{GN}})}{\eta} \right), \tag{4.22}$$

and go on to derive variational principles for model equations that do not suffer from this inconsistency with the conservation laws of the original equations. However, a derivation of the GN equation via an asymptotic expansion similar to (2.39), adopted in deriving the GL equations (see also [6,15]) shows that the proper interpretation of the field $\boldsymbol{u}$ in (4.18) is that of the vertically averaged horizontal velocity of the original Euler model. The columnar motion ansatz (4.10) is only the leading order condition in the expansion of the velocity, and its horizontal components depend weakly (at order $\mathrm{O}(\delta^2)$) on z. This implies that the operation of taking a curl does not commute with that of taking a vertical average, which is ultimately the reason for the appearance of the extra vertical vorticity term Ω^*_{GN} (cf. [8] for the analogous situation within the GL system).

Advection of the potential vorticity $\Omega_{\mathrm{GN}}/\eta$, combined with the continuity relation for η and tangential boundary conditions on the mean velocity $\boldsymbol{u}$, yields an infinity of conserved quantities (cf. Eq. (3.26)),

$$C_\Phi = \int \mathrm{d}x\,\mathrm{d}y\,\eta\Phi\left(\frac{\Omega_{\mathrm{GN}}}{\eta}\right), \tag{4.23}$$

for any function Φ. As for the GL equations, the set of conservation laws C_Φ are Casimir functions for the Lie-Poisson bracket (3.24).

Thus, the Hamiltonian formulations of the GN equations (4.4) and the GL equations (3.1) differ only in the role played in the corresponding Hamiltonians by the surface height h, which enters in the potential energy for H_{GN} in (4.15) and as a Lagrange multiplier in H_{GL} in (3.21). An important consequence of this difference is that it leads to *quadratic* conservation laws for energy and enstrophy for the GL equations, which will be used in Section 6.

5. An explicit flow for the lake equations

Circulation and potential vorticity results analogous to those of Section 3 exist for the leading order system (1.1): these results may be obtained simply by appropriately setting $\delta = 0$ in the results for the GL equations. In the case $\delta = 0$, the operator $-b^{-1}\mathcal{S}(b)$ in (3.39) simplifies considerably. For example, the irrotational steady solutions of (1.1) satisfy

$$-\boldsymbol{\nabla}\cdot((1/b)\boldsymbol{\nabla}\psi)) = 0. \tag{5.1}$$

For the cylindrical symmetric case $b(x, y) = b(r)$, $x = r\cos\theta$, $y = r\sin\theta$ this equation can be solved by separation of variables,

$$\psi(r,\theta) = R(r)\Theta(\theta) \tag{5.2}$$

and the resulting equations for R and Θ are

$$\frac{\mathrm{d}^2\Theta}{\mathrm{d}\theta^2} = -k^2, \quad \text{and} \quad \frac{\mathrm{d}}{\mathrm{d}r}\left(\frac{r}{b}\frac{\mathrm{d}R}{\mathrm{d}r}\right) - \frac{k^2}{rb}R = 0. \tag{5.3}$$

For a flow uniform at $r = \infty$ in the x-direction, we find for the separation constant $k = 1$ so that

$$\Theta(\theta) = \sin\theta \tag{5.4}$$

and impose the boundary conditions on R

$$R(0) = 0, \quad \text{and} \quad R \to R_\infty r \quad \text{as } r \to \infty, \tag{5.5}$$

which corresponds by (3.38) to a uniform velocity at infinity $(u, v) = (R_\infty/b(\infty), 0)$. Closed form solutions for R in (5.3) with nontrivial bottom topographies $b(r)$ can be easily found by casting the R-equation in Schrfödinger-like form via a transformation of variables, and defining the bottom function $\mathcal{B}$ in the transformed variable. For instance, introducing

$$\mathrm{d}\varrho = \frac{b(r)}{r}\,\mathrm{d}r, \qquad \mathcal{B}(\varrho) = b(r(\varrho)), \qquad \mathcal{R}(\varrho) = R(r(\varrho)), \tag{5.6}$$

the R-equation is simply

$$\frac{\mathrm{d}^2\mathcal{R}}{\mathrm{d}\varrho^2} - \frac{\mathcal{R}}{\mathcal{B}^2} = 0. \tag{5.7}$$

The choice of a bottom profile of the form

$$\mathcal{B}(\varrho) = 1/\sqrt{4 - 2\,\mathrm{sech}^2\varrho} \tag{5.8}$$

allows a solution for $\mathcal{R}(\varrho)$ to be given in terms of hyperbolic functions. In the original (physical) variables, r, θ the bottom topography corresponding to the choice (5.8) for b is represented in Fig. 2. The bottom is asymptotically flat at infinity, where the uniform depth is $b = \frac{1}{2}$. The depth initially increases for (x, y) approaching the region around the origin, and it reaches the maximum depth of $b = 1$ on a circle of radius $r = r(0)$. From this bottom depression a cone-like mountain emerges, with the vertex of the cone located at the origin, where $b(0) = b(\infty)$. The radial variable r is defined implicitly through ϱ by the first equation in (5.6), which for the form of $\mathcal{B}$ chosen is

$$r(\varrho) = \exp\left[2\varrho - \sqrt{2}\sinh^{-1}(\tanh\varrho) + \sqrt{1+\tanh^2\varrho}\,\log\left(\frac{1+\sqrt{2}+\tanh\varrho}{1+\sqrt{2}-\tanh\varrho}\right)\right]. \tag{5.9}$$

Here $\varrho \in (-\infty, \infty)$ and r is normalized so that $r(\varrho) \to \mathrm{e}^{2\varrho}$ as $\varrho \to \infty$, and so $r(0) = 1$. By choosing $R_\infty = 1$, the solution R corresponding to the present choice of bottom topography is

$$\mathcal{R}(\varrho) = 2\cosh^2(\varrho) + \sinh(\varrho)\cosh(\varrho)\left[3 - \tanh^2(\varrho)\right], \tag{5.10}$$

so that the uniform velocity at infinity is $(u, v) = (2, 0)$. Hence, from (5.10) the boundary conditions (5.5) are satisfied as $\varrho \to -\infty$ and $\varrho \to \infty$. The streamlines (particle paths) corresponding to the streamfunction

$$\psi(r, \theta) = R(r)\sin\theta = \text{const.} \tag{5.11}$$

are depicted in Fig. 3. As the figure shows, for the irrotational flow of this example the effect of the bottom is to bend the particle paths *towards* the origin, a sort of Venturi effect due to the higher fluid velocities in the shallower regions. This can be checked directly by looking at the "pressure" distribution gh, which for irrotational flows of (1.1) is given by the same expression as for the case of two-dimensional Euler equations, i.e.,

$$gh = -\frac{1}{2}|\boldsymbol{u}|^2 + \text{const.} = -\frac{1}{2b^2}\left[\frac{R^2}{r^2}\cos^2\theta + \left(\frac{\mathrm{d}R}{\mathrm{d}r}\right)^2\sin^2\theta\right] + \text{const.} \tag{5.12}$$

Notice that the original three-dimensional flow that (1.1) approximates has, in the symmetry plane (x, z), a complex velocity potential with a singularity at the tip of the cone (see [2, p. 411]) as $(x + \mathrm{i}z)^\beta$. Here β can be found in terms of the cone angle to be $\beta = \pi/(\pi + 2\arctan 2) < 1$. This leads, by the Bernoulli expression for the pressure, to an infinite negative pressure at the cone tip. The effect of this singularity in the three-dimensional flow is actually exhibited by Eq. (1.1). The value of the pressure at the origin is, by (5.12), $gh = -2\lim_{\varrho\to-\infty}\mathcal{R}^2/r^2$, which is about 10 times higher than the pressure at infinity where $gh = -2$. This leads to the strong convergence of the streamlines towards the origin that can be seen in Fig. 3.

We remark that in choosing the depth function b and velocity at infinity for this example no attention has been paid to the scaling assumptions under which the lake equations (1.1) are derived. Thus, the value of h at the origin turns out to be $h(0) < -b(0)$ which is inconsistent with the definition of h. This offers an example for the discussion in Section 3 on the need to choose initial data (and boundary conditions) for the dimensional form of lake and GL equations which are in agreement with the scaling assumptions (2.1)–(2.4). In the context of this example, the appropriate scaling of R_∞ is needed so that the velocity at infinity is small compared to $\sqrt{g/2}$ (or $2R_\infty/\sqrt{g/2} \ll 1$).

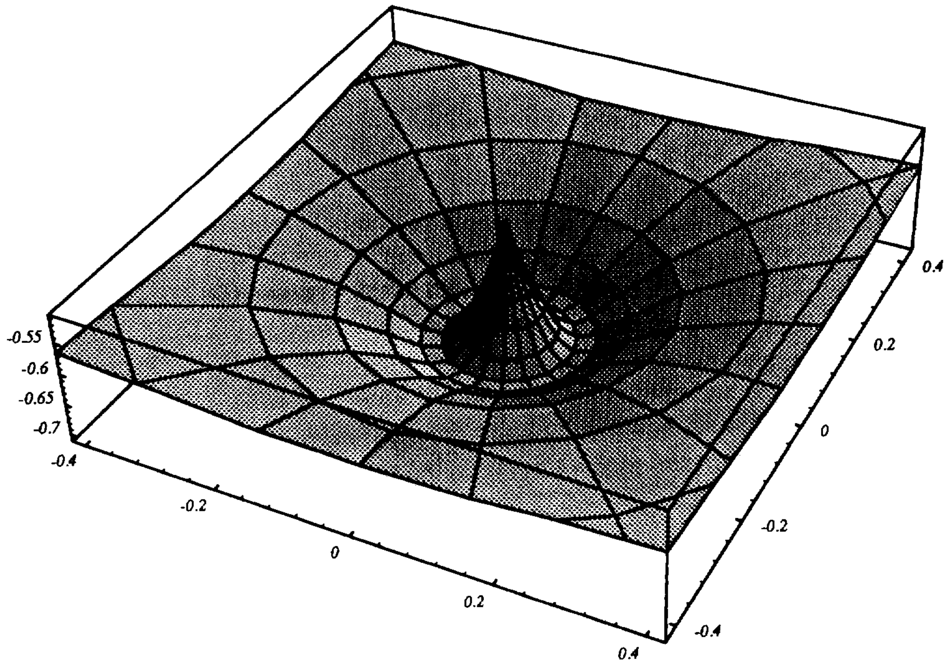

Fig. 2. The bottom topography $b(x, y)$ given by the choice (5.8) and the definition (5.6).

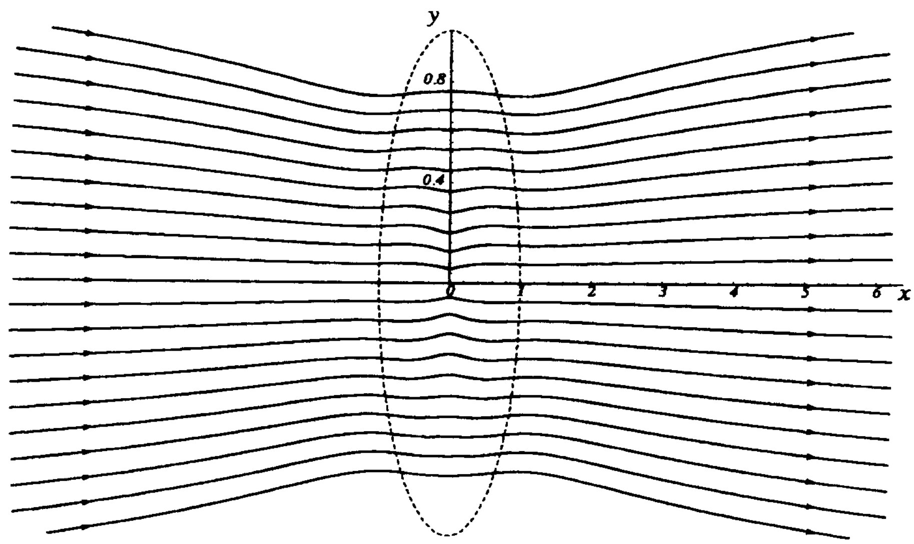

Fig. 3. Plot of the streamlines near the origin for the steady flow determined by the solution ψ of (5.1) with the bottom topography depicted in Fig. 2. The dashed curve represents the location of the circle of maximum depth $4 = 1$. The elongation in the y-direction is an artifact of the different scaling for the x- and y-axis, so chosen to emphasize the convergence of the streamlines towards the origin.

6. Bounding the deviation between solutions

We now bound the deviation of the solutions of the GL equations (1.2) from the solutions of the leading order lake equations (1.1), starting from the same initial conditions for mean horizontal velocity. That is, we bound the effect of hydrostatic imbalance and topographic forcing on the solution over long times. To do this, we rewrite the lake equations as

$$\partial_t \boldsymbol{u}^{(0)} + \boldsymbol{u}^{(0)} \cdot \boldsymbol{\nabla} \boldsymbol{u}^{(0)} - (\boldsymbol{\nabla} \boldsymbol{u}^{(0)})\boldsymbol{u}^{(0)} = -\boldsymbol{\nabla}\left(gh^{(0)} + \tfrac{1}{2}|\boldsymbol{u}^{(0)}|^2\right) \equiv -\boldsymbol{\nabla} P^{(0)}, \qquad \boldsymbol{\nabla}\cdot\left(b\boldsymbol{u}^{(0)}\right) = 0, \tag{6.1}$$

and the GL equations as

$$\partial_t \boldsymbol{v} + \boldsymbol{u} \cdot \boldsymbol{\nabla} \boldsymbol{v} - (\boldsymbol{\nabla} \boldsymbol{v})\boldsymbol{u} = -\boldsymbol{\nabla}\left(gh - \tfrac{1}{2}|u|^2 + \boldsymbol{v}\cdot\boldsymbol{u}\right) \equiv -\boldsymbol{\nabla} P, \qquad \boldsymbol{\nabla}\cdot(b\boldsymbol{u}) = 0, \tag{6.2}$$

where $b\boldsymbol{v} = \mathcal{L}(b)\boldsymbol{u}$. The corresponding energies are

$$H^{(0)} = \frac{1}{2}\int \mathrm{d}x\,\mathrm{d}y b|\boldsymbol{u}^{(0)}|^2, \quad \text{and} \quad H = \frac{1}{2}\int \mathrm{d}x\,\mathrm{d}y b\boldsymbol{u}\cdot\boldsymbol{v}, \tag{6.3}$$

each of which is a positive-definite quadratic form. These energies may be shown to be conserved by integrating the scalar product of the first equation in (6.1) with $b\boldsymbol{u}^{(0)}$ and the first equation in (6.2) with $b\boldsymbol{u}$ over the $\boldsymbol{x}$-domain. The result follows in each case upon integrating by parts using the weighted divergence conditions, and requiring that $\boldsymbol{u}$ and $\boldsymbol{u}^{(0)}$ are both tangent to the boundary.

Taking the difference of the same scalar products gives the equation

$$b\left(\boldsymbol{u} - \boldsymbol{u}^{(0)}\right) \cdot \partial_t \left(\boldsymbol{v} - \boldsymbol{u}^{(0)}\right) = \mathrm{RHS}, \tag{6.4}$$

where

$$\mathrm{RHS} \equiv b\left(\boldsymbol{u} \times \boldsymbol{u}^{(0)}\right) \boldsymbol{\nabla} \times \left(\boldsymbol{v} - \boldsymbol{u}^{(0)}\right) - \boldsymbol{\nabla}\cdot\left[\left(P - P^{(0)}\right) b \left(\boldsymbol{u} - \boldsymbol{u}^{(0)}\right)\right]. \tag{6.5}$$

Consequently,

$$\left(\boldsymbol{u} - \boldsymbol{u}^{(0)}\right) \cdot \mathcal{L}(b)\partial_t \left(\boldsymbol{u} - \boldsymbol{u}^{(0)}\right) + \left(\boldsymbol{u} - \boldsymbol{u}^{(0)}\right) \cdot (\mathcal{L}(b) - b\mathbf{1}) \cdot \partial_t \boldsymbol{u}^{(0)} = \mathrm{RHS}, \tag{6.6}$$

and integration over the $\boldsymbol{x}$-domain gives

$$\begin{aligned}
&\frac{1}{2}\frac{\mathrm{d}}{\mathrm{d}t}\int \mathrm{d}x\,\mathrm{d}y \left(\boldsymbol{u} - \boldsymbol{u}^{(0)}\right) \cdot \mathcal{L}(b) \left(\boldsymbol{u} - \boldsymbol{u}^{(0)}\right) \\
&\quad = \int \mathrm{d}x\,\mathrm{d}y \mathrm{RHS} - \int \mathrm{d}x\,\mathrm{d}y \left(\boldsymbol{u} - \boldsymbol{u}^{(0)}\right) \cdot (\mathcal{L}(b) - b\mathbf{1})\, \partial_t \boldsymbol{u}^{(0)} \\
&\quad \le \int \mathrm{d}x\,\mathrm{d}y \mathrm{RHS} + \int \mathrm{d}x\,\mathrm{d}y |\boldsymbol{u} - \boldsymbol{u}^{(0)}|\,|(\mathcal{L}(b) - b\mathbf{1})\, \partial_t \boldsymbol{u}^{(0)}| \\
&\quad \le \int \mathrm{d}x\,\mathrm{d}y \mathrm{RHS} \\
&\qquad + \left(\int \mathrm{d}x\,\mathrm{d}y \left(\boldsymbol{u} - \boldsymbol{u}^{(0)}\right) \cdot \mathcal{L}(b) \left(\boldsymbol{u} - \boldsymbol{u}^{(0)}\right)\right)^{1/2} \left(\int \mathrm{d}x\,\mathrm{d}y b^{-1} |(\mathcal{L}(b) - b\mathbf{1})\, \partial_t \boldsymbol{u}^{(0)}|^2\right)^{1/2},
\end{aligned} \tag{6.7}$$

where we have used the Schwarz inequality in the last step. Hence, by introducing the functionals

$$\mathcal{H}(t) = \frac{1}{2}\int \mathrm{d}x\,\mathrm{d}y\left(\boldsymbol{u}-\boldsymbol{u}^{(0)}\right)\cdot\mathcal{L}(b)\left(\boldsymbol{u}-\boldsymbol{u}^{(0)}\right),$$
$$F(t) = \frac{1}{2}\int \mathrm{d}x\,\mathrm{d}y b^{-1}\left|(\mathcal{L}(b)-b\mathbf{1})\cdot\partial_t\boldsymbol{u}^{(0)}\right|^2, \tag{6.8}$$

we have

$$\frac{\mathrm{d}}{\mathrm{d}t}\mathcal{H} \le \int \mathrm{d}x\,\mathrm{d}y\mathrm{RHS} + 2\sqrt{\mathcal{H}F}. \tag{6.9}$$

The energy norm $\mathcal{H}(t)$ bounds the square of the L_2 norm $\|\boldsymbol{u}-\boldsymbol{u}^{(0)}\|$,

$$2\mathcal{H} \ge \int \mathrm{d}x\,\mathrm{d}y b\left|\boldsymbol{u}-\boldsymbol{u}^{(0)}\right|^2, \tag{6.10}$$

since $\mathcal{L}(b) - b\mathbf{1}$ is a positive-definite operator (cf. (3.34), (3.35) and (3.5)). The integral $\int$ dx dyRHS is estimated as follows,

$$\begin{aligned}\int \mathrm{d}x\,\mathrm{d}y\mathrm{RHS} &\le \int \mathrm{d}x\,\mathrm{d}y b^2\left|\boldsymbol{u}-\boldsymbol{u}^{(0)}\right|\left|\boldsymbol{u}^{(0)}\right|\left|b^{-1}\boldsymbol{\nabla}\times\left(\boldsymbol{v}-\boldsymbol{u}^{(0)}\right)\right| \\ &\le \sup_t\left|b\boldsymbol{u}^{(0)}\right|\int \mathrm{d}x\,\mathrm{d}y b\left|\boldsymbol{u}-\boldsymbol{u}^{(0)}\right|\left|b^{-1}\boldsymbol{\nabla}\times\left(\boldsymbol{v}-\boldsymbol{u}^{(0)}\right)\right| \\ &\le \sup_t\left|b\boldsymbol{u}^{(0)}\right|\left(\int \mathrm{d}x\,\mathrm{d}y b\left|\boldsymbol{u}-\boldsymbol{u}^{(0)}\right|^2\right)^{1/2}\left(\int \mathrm{d}x\,\mathrm{d}y b(\Omega/b-\omega/b)^2\right)^{1/2} \\ &\le 2\sup_t\left|b\boldsymbol{u}^{(0)}\right|\sqrt{\mathcal{H}\mathcal{E}} \equiv 2C_1\sqrt{\mathcal{H}\mathcal{E}},\end{aligned} \tag{6.11}$$

with enstrophy of the difference, $\mathcal{E}$, given by

$$\mathcal{E} = \frac{1}{2}\int \mathrm{d}x\,\mathrm{d}y b(\Omega/b-\omega/b)^2, \tag{6.12}$$

where we have used (6.10) to get the last inequality. Here and in the following we write $\omega \equiv \omega_3^{(0)}$ for ease of notation. Similarly, we obtain the following estimate from the weighted divergence conditions and tangential boundary conditions on $\boldsymbol{u}$ and $\boldsymbol{u}^{(0)}$, the advection relation (3.9) and the corresponding relation for ω/b,

$$\begin{aligned}\frac{\mathrm{d}}{\mathrm{d}t}\mathcal{E} &= -\int \mathrm{d}x\,\mathrm{d}y b(\Omega/b-\omega/b)\left(\boldsymbol{u}\cdot\boldsymbol{\nabla}\Omega/b-\boldsymbol{u}^{(0)}\cdot\boldsymbol{\nabla}\omega/b\right) \\ &= -\int \mathrm{d}x\,\mathrm{d}y b(\Omega/b-\omega/b)\left(\boldsymbol{u}-\boldsymbol{u}^{(0)}\right)\cdot\boldsymbol{\nabla}(\omega/b) \\ &\le \sup_t|\boldsymbol{\nabla}(\omega/b)|\int \mathrm{d}x\,\mathrm{d}y b\left|\boldsymbol{u}-\boldsymbol{u}^{(0)}\right||\Omega/b-\omega/b| \\ &\le 2\sup_t|\boldsymbol{\nabla}(\omega b)|\sqrt{\mathcal{H}\mathcal{E}} \equiv 2C_2\sqrt{\mathcal{H}\mathcal{E}}.\end{aligned} \tag{6.13}$$

Combining (6.9), (6.11) and (6.13) gives

$$\frac{\mathrm{d}}{\mathrm{d}t}\left(\sqrt{\mathcal{H}}+\sqrt{\mathcal{E}}\right) \le C_1\sqrt{\mathcal{E}} + C_2\sqrt{\mathcal{H}} + \sqrt{\mathcal{F}} \le C_3\left(\sqrt{\mathcal{H}}+\sqrt{\mathcal{E}}\right) + \sqrt{F}, \tag{6.14}$$

where

$$C_1 = \sup_t |bu^{(0)}|, \qquad C_2 = \sup_t |\nabla(\omega/b)|, \qquad C_3 = \max\{C_1, C_2\}. \tag{6.15}$$

Consequently, the Gronwall inequality gives

$$\sqrt{\mathcal{H}(t)} + \sqrt{\mathcal{E}(t)} \le e^{C_3 t}\left[\sqrt{\mathcal{H}(0)} + \sqrt{\mathcal{E}(0)} + \int^t dt' e^{-C_3 t'}\sqrt{F(t')}\right], \tag{6.16}$$

for the energy/enstrophy norm of the difference of the solutions. According to the estimate (6.16), the factors in the reference solution that drive the deviation away from the hydrostatic approximation are its velocity (C_1) and the *gradient* of its potential vorticity (C_2), as well as its accelerations occurring at high wave numbers ($F(t)$). The quantity $F(t)$ is $O(\delta^2)$. So, if the initial deviation from the reference solution is $O(\delta^2)$, or less, then the norm of the deviation from the reference solution at a later time, $\mathcal{N}(t)$, with

$$\mathcal{N}(t) = \sqrt{\mathcal{H}(t)} + \sqrt{\mathcal{E}(t)}, \tag{6.17}$$

cannot be of order one before a time of order $O(\log(1/\delta^2))$ has elapsed.

Therefore, given a hydrostatic reference solution $u^{(0)}(x, t)$, we may estimate the norm $\mathcal{N}(t)$ of the difference of solutions due to hydrostatic imbalance and topographic forcing as a function of time, initial conditions and the reference solution. As measured by this norm, the estimate (6.16) provides an upper bound on how rapidly hydrostatic imbalance and topographic forcing invalidate the hydrostatic approximation in the present scaling regime. According to this estimate, there are two factors driving the deviation from the hydrostatic approximation. First, the higher the momentum and potential vorticity gradient of the initial condition, the more quickly the flows can depart from the hydrostatic approximation. Second, the stronger the accelerations in the hydrostatic reference solution occurring at high wave number (where $F(t)$ is large due to the unboundedness of $\mathcal{L}(b) - b\mathbf{1}$), the more quickly the flows can depart. Both of these factors can lead to exponential growth in slow time T/δ^3 of the $\mathcal{N}(t)$ norm of the difference of solutions. This time scale is comparable to the time taken by a fluid parcel to cross a typical horizontal length scale, and seems to us unexpectedly short for effects of nonhydrostatic pressure to be felt. This indicates either the need for sharper estimates or an example for which the bound is saturated, as might occur in a situation where the nonhydrostatic terms would destabilize the reference flow.

Acknowledgements

We are grateful to Peter Constantin, Mac Hyman, Len Margolin, Edriss Titi, Ted Wu, and Vladimir Zakharov for valuable discussions. This work was partially supported by the US Department of Energy CHAMMP program. We would also like to thank IGPP and CNLS at Los Alamos for their hospitality at the Summer '93 Workshop on Ocean Modeling, where some of this work was completed. Some of this work was carried out while CDL was visiting the Center for Nonlinear Studies (CNLS) at Los Alamos National Laboratory, which is supported in part by the DOE under grant W7404-ENG-36.

References

[1] V.I. Arnold, Conditions for nonlinear stability of the plane curvilinear flows of an ideal fluid, Dok. Mat. Nauk 162 (5) (1965) 773–777.
[2] G.K. Batchelor, An Introduction to Fluid Mechanics (Cambridge University Press, London, 1985).
[3] B.J. Bayly, C.D. Levermore and T. Possot, Density variations in a weakly compressible fluid flow, Phys. Fluids A 4 (1991) 945–954.

[4] S.V. Bazdenkov, N.N. Morozov and O.P. Pogutse, Dispersive effects in two-dimensional hydrodynamics, Dokl. Akad. Nauk SSSR 293 (1985) 818–822; [Soviet Phys. Dokl. 32 (1985) 262–264].
[5] D.J. Benny, Some properties of long nonlinear waves, Stud. Appl. Math. 52 (1973) 45–50.
[6] W. Choi and R. Camassa, Weakly nonlinear internal waves in a two-fluid system, J. Fluid Mech. 313 (1992) 83–103.
[7] R. Camassa and D.D. Holm, Dispersive barotropic equations for stratified mesoscale ocean dynamics, Physica D 60 (1992) 1–15.
[8] R. Camassa, C.D. Levermore and D.D. Holm, Long time shallow water equations with a varying bottom, J. Fluid Mech. (1994) submitted.
[9] A.E. Green and P.M. Naghdi, A derivation of equations for wave propagation in water of variable depth, J. Fluid Mech. 78 (1976) 237–246.
[10] D.D. Holm, Hamiltonian structure for two-dimensional hydrodynamics with nonlinear dispersion, Phys. Fluids 31 (1988) 2371–2373.
[11] D.D. Holm, B.A. Kupershmidt and C.D. Levermore, Canonical maps between Poisson brackets in Eulerian and Langrangian descriptions of continuum mechanics, Phys. Lett. A 98 (1983) 389–395.
[12] D.D. Holm, J.E. Marsden and T.S. Ratiu, Hamiltonian Structure and Lyapunov Stability for Ideal Continuum Dynamics, University of Montreal Press, Montreal, 1985).
[13] D.D. Holm, J.E. Marsden, T. Ratiu and A. Weinstein, Nonlinear stability of fluid and plasma equilibria, Phys. Rep. 123 (1985) 1–116.
[14] C.D. Levermore, M. Oliver and E.S. Titi, Global well-posedness for certain shallow water equations with a varying bottom, Ind. Univ. Math. J. (1995) submitted; Global well-posedness for the lake equations, Physica D 98 (1996) 492–509, these Proceedings.
[15] L.G. Margolin, B.T. Nadiga and P.K. Smolarkiewicz, Various approximations of the shallow flow over an obstacle, Phys. Fluids, submitted.
[16] J. Miles and R. Salmon, Weakly dispersive nonlinear gravity waves, J. Fluid Mech. 157 (1985) 519–531.
[17] R.D. Smith, J.K. Dukowitz and R.C. Malone, Parallel ocean general circulation modeling, Physica D 60 (1992) 38–60.
[18] C.H. Su and C.S. Gardner, Korteweg–de Vries equation and generalization III: Derivation of the Korteweg–de Vries equation and Burgers equation, J. Math. Phys. 10 (1969) 536–539.
[19] V.E. Zakharov, On the Benny equations, Physica D 3 (1981) 193–202.